Neurosci Bull October 1, 2014, 30(5): 777–811. http://www.neurosci.cn
DOI: 10.1007/s12264-014-1460-6

·Review·

Development of ^{18}F-labeled radiotracers for neuroreceptor imaging with positron emission tomography

Peter Brust, Jörg van den Hoff, Jörg Steinbach

Helmholtz-Zentrum Dresden-Rossendorf, Institute of Radiopharmaceutical Cancer Research, Permoserstrasse 15, Leipzig 04318, Germany

Corresponding author: Peter Brust. E-mail: p.brust@hzdr.de

Positron emission tomography (PET) is an *in vivo* molecular imaging tool which is widely used in nuclear medicine for early diagnosis and treatment follow-up of many brain diseases. PET uses biomolecules as probes which are labeled with radionuclides of short half-lives, synthesized prior to the imaging studies. These probes are called radiotracers. Fluorine-18 is a radionuclide routinely used in the radiolabeling of neuroreceptor ligands for PET because of its favorable half-life of 109.8 min. The delivery of such radiotracers into the brain provides images of transport, metabolic, and neurotransmission processes on the molecular level. After a short introduction into the principles of PET, this review mainly focuses on the strategy of radiotracer development bridging from basic science to biomedical application. Successful radiotracer design as described here provides molecular probes which not only are useful for imaging of human brain diseases, but also allow molecular neuroreceptor imaging studies in various small-animal models of disease, including genetically-engineered animals. Furthermore, they provide a powerful tool for *in vivo* pharmacology during the process of pre-clinical drug development to identify new drug targets, to investigate pathophysiology, to discover potential drug candidates, and to evaluate the pharmacokinetics and pharmacodynamics of drugs *in vivo.*

Keywords: Alzheimer's disease; autoradiography; blood-brain barrier; brain tumor; cholinergic system; kinetic modeling; metabolism; molecular imaging; neurodegeneration; positron emission tomography; precursor; psychiatric disorder; radiotracer; sigma receptor

Introduction

Positron emission tomography (PET) is an *in vivo* molecular imaging tool widely used in nuclear medicine for early diagnosis and treatment follow-up of many brain diseases. Positron-emitting radionuclide-labeled substances allow the visualization, characterization, and measurement of biological processes at the molecular and cellular levels in humans and other living systems by highly sensitive coincidence-detection[1]. This is based on 511 keV photons (gamma radiation) originating from positron-electron annihilation. PET differs in that aspect from other modalities such as single-photon emission computed tomography (SPECT), magnetic resonance imaging (MRI), optical imaging, and ultrasound. Because of their high sensitivity (~10^{-9} to 10^{-12} M) PET and SPECT offer advantages over the other methods. Therefore, in the past, they were the only modalities that allowed noninvasive imaging of biochemical receptor sites. Nowadays, the other imaging modalities compete in that aspect although precise absolute quantitation in terms of biochemical parameters has not been achieved yet.

Recently, multimodal imaging approaches, specifically PET/CT and PET/MRI, have been suggested to bring a new perspective into the fields of clinical and preclinical imaging. Clinical cases have shown that the combination of anatomical structures, revealed by CT and MRI, and the functional information from PET into one image, with high

fusion accuracy, provides an advanced diagnostic tool and research platform[2, 3].

PET and SPECT use biomolecules as probes, labeled with radionuclides of short half-lives, synthesized prior to the imaging studies. These probes are called radiotracers. According to the concept developed by George von Hevesy[4] a radiotracer is a chemical compound in which one or more atoms have been replaced by its radioisotope. By virtue of its radioactive decay, it can be used to follow the original compound as it acts in the same manner. Due to the extremely small concentrations required, the radiotracer does not disturb the systemic processes to be studied. This allows the tracing of chemical, biochemical, and physiological processes and investigation of their functions and capacities.

Although SPECT is the most common imaging tool in clinical nuclear medicine, this review is focused on PET. SPECT primarily uses radioiodine, e.g. ^{123}I, or radiometals, e.g. ^{99m}Tc as the label. Iodine is rarely present and metals are usually absent from the protein-binding drugs that serve as lead structures. Therefore, the applicability of SPECT for neuroimaging is rather limited, because labeling with ^{123}I or ^{99m}Tc causes strong and unpredictable alterations of target affinities and blood-brain-barrier (BBB) permeability. The positron-emitting radionuclides ^{11}C and ^{18}F, introduced as an isotopic modification (^{11}C for ^{12}C; "isotopic labeling") or an atomic substitute (^{18}F for ^{1}H, OH; "isosteric, isoelectronic, or bioisosteric labeling"), generate rather small affinity changes, if any. ^{18}F is considered the most suitable radionuclide for PET because of its five-fold longer half-life (109.8 min) than ^{11}C, its high β^+ yield (97%) and its lower positron energy maximum of 640 keV (IAEA, Nuclear Data Services, https://www-nds.iaea.org/relnsd/vcharthtml/VChartHTML.html).

Despite the limitations, the principles and strategies for radiotracer development described below also apply to SPECT. Also, aspects of radiation safety, toxicology issues, quality control, licensing, and regulatory control, which need to be considered for the production of radiopharmaceuticals suitable for administration to humans, have been reviewed extensively elsewhere[5]. Meanwhile, a highly regulated system for radiopharmaceutical production has been established in most of the developed countries (http://ec.europa.eu/health/documents/eudralex/vol-4/index_en.htm). This topic is therefore excluded from further consideration.

Successful radiotracer design as described below does not necessarily lead to human application. Nowadays, special PET and SPECT devices are available for small-animal imaging, allowing molecular neuroreceptor imaging studies in various models of disease including genetically-engineered animals[6, 7]. They provide a powerful tool for *in vivo* pharmacology during the process of pre-clinical drug development to identify new drug targets, to investigate pathophysiology, to discover potential drug candidates, and to evaluate the pharmacokinetics and pharmacodynamics of drugs *in vivo*[8].

The general sequence of radiotracer development is shown in Fig. 1 and can be followed up in a short video available at http://www.beilstein.tv/tvpost/toxic-epibatidine-was-structurally-modified-to-image-alzheimer%C2%B4s-disease/. This demonstrates how chemical/pharmaceutical and biochemical/pharmacological steps interact to finally decide whether to break-off or continue the development process. PET radiotracers that have been developed for neuroreceptor imaging and have already been used in humans are listed in Table 1.

Target Selection and Identification of Lead Structures

Careful selection of the target to be imaged in combination

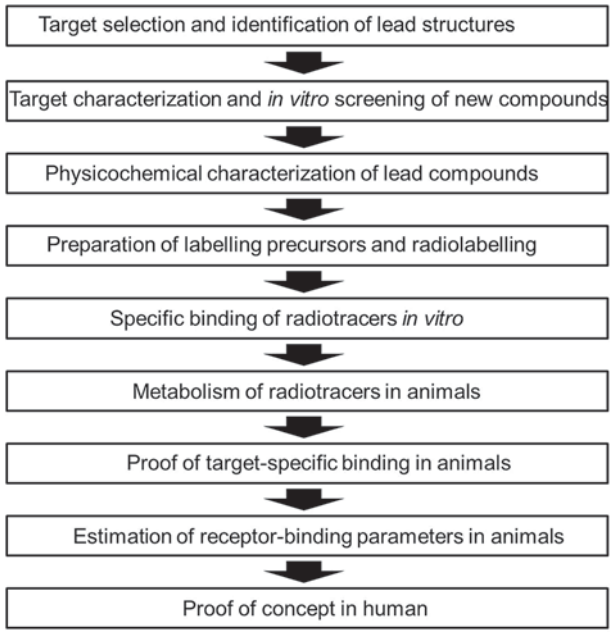

Fig. 1. Strategy for development of new PET radiotracers for neuroimaging.

Table 1. Neuroreceptor targets[a] that have been used for successful PET radiotracer development

Neuroreceptor	PET radiotracer	Selected reference for human use
Acetylcholine receptor: muscarinic	[^{11}C]scopolamine	Frey *et al.* 1992[9]
Acetylcholine receptor: muscarinic	[N-^{11}C-methyl]-benztropine	Xie *et al.* 2004[10]
Acetylcholine receptor: muscarinic	[^{11}C](+)3-MPB	Yamamoto *et al.* 2012[11]
Acetylcholine receptor: muscarinic M2	[^{18}F]FP-TZTP	Ichise *et al.* 2008[12]
Acetylcholine receptor: nicotinic α4β2	2-[^{18}F]fluoro-A-85380	Sabri *et al.* 2008[13]
Acetylcholine receptor: nicotinic α4β2	6-[^{18}F]fluoro-A-85380	Ding *et al.* 2004[14]
Acetylcholine receptor: nicotinic α4β2	[^{18}F]AZAN	Wong *et al.* 2013[15]
Acetylcholine receptor: nicotinic α4β2	(-)-[^{18}F]flubatine	Sabri *et al.* 2011[16]
Acetylcholine receptor: nicotinic α7	[^{11}C]CHIBA-1001	Toyohara *et al.* 2009[17]
Adenosine receptor: A_1	[^{18}F]CPFPX	Bauer *et al.* 2003[18]
Adenosine receptor: A_1	[^{11}C]MPDX	Fukumitsu *et al.* 2008[19]
Adenosine receptor: A_{2A}	[^{11}C]TMSX	Mishina *et al.* 2011[20]
Adenosine receptor: A_{2A}	[^{11}C]SCH442416	Ramlackhansingh *et al.* 2011[21]
Cannabinoid receptor: CB_1	[^{18}F]MK-9470	Burns *et al.* 2007[22]
Cannabinoid receptor: CB_1	[^{11}C]MePPEP	Terry *et al.* 2010[23]
Cannabinoid receptor: CB_1	[^{18}F]FMPEP-d	Terry *et al.* 2010[23]
Cannabinoid receptor: CB_1	[^{11}C]OMAR	Wong *et al.* 2010[24]
Cannabinoid receptor: CB_2	[^{11}C]NE40	Ahmad *et al.* 2013[25]
Dopamine receptor: D_1	[^{11}C]SCH 23390	Farde *et al.* 1987[26]
Dopamine receptor: D_1	[^{11}C]NNC687	Karlsson *et al.* 1993[27]
Dopamine receptor: D_1	[^{11}C]NNC756	Karlsson *et al.* 1993[27]
Dopamine receptor: D_1	[^{11}C]NNC112	Slifstein *et al.* 2008[28]
Dopamine receptor: D_2-D_3	[^{11}C]raclopride	Farde *et al.* 1986[29]
Dopamine receptor: D_2-D_3	[^{11}C]NMSP	Wong *et al.* 1986[30]
Dopamine receptor: D_2-D_3	[^{11}C]NPA	Narendran *et al.* 2009[31]
Dopamine receptor: D_2-D_3	[^{11}C]MNPA	Otsuka *et al.* 2009[32]
Dopamine receptor (extrastriatal): D_2/D_3	[^{11}C]FLB457	Farde *et al.* 1997[33]
Dopamine receptor (extrastriatal): D_2/D_3	[^{18}F]fallypride	Mukherjee *et al.* 2002[34]
Dopamine receptor: D_3>D_2	[^{11}C]-(+)-PHNO	Ginovart *et al.* 2007[35]
Estrogen receptor	[^{18}F]FES	Moresco *et al.* 1997[36]
Glutamate receptor: mGluR1	[^{11}C]ITMM	Toyohara *et al.* 2013[37]
Glutamate receptor: mGluR5	[^{11}C]ABP688	Ametamey *et al.* 2007[38]
Glutamate receptor: mGluR5	[^{18}F]SP203	Brown *et al.* 2008[39]
Glutamate receptor: mGluR5	[^{11}C]AZD9272	Kagedal *et al.* 2012[40]
Glutamate receptor: mGluR5	[^{18}F]FPEB	Wong *et al.* 2013[41]
Glutamate NMDA receptor: PCP site	[^{11}C]ketamine	Kumlien *et al.* 1999[42]
Glutamate NMDA receptor: PCP site	[^{11}C]CNS-5161	Hammers *et al.* 2004[43]
Glutamate NMDA receptor: PCP site	[^{18}F]fluoromemantine	Ametamey *et al.* 2002[44]
Glutamate NMDA receptor: PCP site	[^{18}F]GE-179	McGinnity *et al.* 2014[45]
Glutamate NMDA receptor: glycine-site	[^{11}C]AcL703	Matsumoto *et al.* 2007[46]
Histamine receptor: H1	[^{11}C]doxepin	Yanai *et al.* 1991[47]

(To be continued)

(Continued)

Histamine receptor: H3	[^{11}C]GSK189254	Ashworth *et al.* 2010[48]
GABA-benzodiazepine receptor: α1	[^{11}C]flumazenil	Persson *et al.* 1985[49]
GABA-benzodiazepine receptor: α1	[^{18}F]fluoroethyl-flumazenil	Leveque *et al.* 2003[50]
GABA-benzodiazepine receptor: α1	[^{18}F]fluoroflumazenil	Lee *et al.* 2007[51]
GABA-benzodiazepine receptor: α1	[^{18}F]flumazenil	Massaweh *et al.* 2009[52]
GABA-benzodiazepine receptor: α5	[^{11}C]Ro15-4513	Lingford-Hughes e al. 2002[53]
Opioid receptor: μ	[^{11}C]carfentanil	Frost *et al.* 1990[54]
Opioid receptor: δ	[^{11}C]methylnaltrindol	Madar *et al.* 1997[55]
Opioid receptor: κ	[^{11}C]GR103545	Tomasi *et al.* 2010[56]
Opioid receptor: unselective	[^{11}C]diprenorphine	Frost *et al.* 1990[54]
Opioid receptor: unselective	[^{18}F]FcyF	Cohen *et al.* 2000[57]
Opioid receptor: unselective	[^{18}F]fluorethyldiprenorphine	Baumgärtner *et al.* 2006[58]
Neuropeptide Y receptor: Subtype 1	[^{18}F]Y1-973	Hostetler *et al.* 2011[59]b
Serotonin receptor: 5-HT$_{1A}$	[^{11}C]WAY-100635	Pike *et al.* 1995[60]
Serotonin receptor: 5-HT$_{1A}$	[carbonyl-^{11}C]WAY-100635	Parsey *et al.* 2000[61]
Serotonin receptor: 5-HT$_{1A}$	[carbonyl-^{11}C]DWAY	Andree *et al.* 2002[62]
Serotonin receptor: 5-HT$_{1A}$	[^{11}C]CPC-222	Houle *et al.* 1997[63]
Serotonin receptor: 5-HT$_{1A}$	[^{11}C]CUMI-101	Milak *et al.* 2010[64]
Serotonin receptor: 5-HT$_{1A}$	[^{18}F]MPPF	Costes *et al.* 2002[65]
Serotonin receptor: 5-HT$_{1A}$	[^{18}F]FCWAY	Theodore *et al.* 2006[66]
Serotonin receptor: 5-HT$_{1B}$	[^{11}C]P943	Gallezot *et al.* 2010[67]
Serotonin receptor: 5-HT$_{1B}$	[^{11}C]AZ10419369	Varnäs *et al.* 2011[68]
Serotonin receptor: 5-HT$_{1B}$	[^{11}C]P943	Murrough *et al.* 2011[69]
Serotonin receptor: 5-HT$_{2A}$	[^{11}C]MDL100907	Hinz *et al.* 2007[70]
Serotonin receptor: 5-HT$_{2A}$	[^{18}F]altanserin	Rosier *et al.* 1996[71]
Serotonin receptor: 5-HT$_{2A}$	[^{18}F]deuteroaltanserin	Van Dyck *et al.* 2000[72]
Serotonin receptor: 5-HT$_{2A}$	[^{18}F]setoperone	Trichard *et al.* 1998[73]
Serotonin receptor: 5-HT$_{2A}$	[^{18}F]Cimbi-36	Ettrup *et al.* 2014[74]
Serotonin receptor: 5-HT$_{4}$	[^{11}C]SB207145	Marner *et al.* 2009[75]
Serotonin receptor: 5-HT$_{6}$	[^{11}C]GSK215083	Parker *et al.* 2012[76]
Sigma receptor: σ$_1$	[^{11}C]SA4503	Mishina *et al.* 2005[77]
Sigma receptor: σ$_1$	[^{18}F]FPS	Waterhouse *et al.* 2004[78]
Translocator protein (TSPO)[b]	[^{11}C]PK11195	Junck *et al.* 1989[79]
Translocator protein (TSPO)	(*R*)-[^{11}C]PK11195	Banati *et al.* 1999[80]
Translocator protein (TSPO)	[^{11}C]PBR28	Brown *et al.* 2007[81]
Translocator protein (TSPO)	[^{11}C]DPA-713	Endres *et al.* 2009[82]
Translocator protein (TSPO)	[^{11}C]DAA1106	Yasuno *et al.* 2012[83]
Translocator protein (TSPO)	[^{11}C]vinpocetine	Gulyas *et al.* 2012[84]
Translocator protein (TSPO)	[^{18}F]F-PBR06	Fujimura *et al.* 2009[85]
Translocator protein (TSPO)	[^{18}F]DPA-714	Arlicot *et al.* 2012[86]
Translocator protein (TSPO)	[^{18}F]FEPPA	Mizrahi *et al.* 2012[87]
Translocator protein (TSPO)	[^{18}F]PBR-111	Guo *et al.* 2013[88]

[a]Neurotransmitter transporters are not considered; [b]formerly known as peripheral benzodiazepine receptor.

with proper identification of a lead structure and subsequently an appropriate lead compound is one of the most important steps in the process of radiotracer development. Considering the resources needed to obtain a radiopharmaceutical ready for human application, strong biomedical or even pathological relevance of the chosen target is needed. Major groups of brain diseases such as neurodegenerative diseases, affective disorders, and brain tumors are expected to be of multifactorial origin, i.e., interactions between multiple genes influenced by internal and external factors occur, and this may have pathological or protective consequences.

Imaging with a single radiotracer offers the chance of picking out only one dedicated piece of the whole scenario of physiological interactions. Thus, it is important to select those key proteins as rational targets which are predominantly altered in pathophysiological states. Ideally, they are causally involved in the etiology of the disease, providing the possibility that their imaging may have impact on both diagnosis and therapeutic drug development.

A schematic view of this complex situation, identifying important molecules involved in the three classes of diseases noted above, is shown in Fig. 2. Notably, many of them are identical though occurring in different contexts. Therefore, it is highly likely that radiotracers designed, for instance, for imaging a certain key protein in the etiology of Alzheimer´s disease (AD) may also be of major importance for other diseases, which further justifies the efforts expended on radiotracer development.

For example, sigma$_1$ (σ_1) receptors are chaperones involved in the suppression of oxidative stress, a feature that links them to numerous brain diseases[89]. Post-mortem studies have shown loss of σ_1 binding sites in the hippocampus of patients with AD[90] and in the cortex of patients with schizophrenia[91]. Overexpression of σ receptors has been found in many brain tumor cell lines and in human brain tumors[92]. The neuroprotective potential of σ_1 receptor agonists has been shown in different models of neurodegeneration[89, 93] and is expected to be important for cancerous diseases as well[92, 94].

As another example, impaired cholinergic neurotransmission is a key feature of AD and the related cognitive impairment is at least partially associated with loss of cortical nicotinic acetylcholine receptors (nAChRs)[6, 95]. There is evidence that both subtypes with the highest expression in the brain are involved: α4β2 and α7 nAChRs. Accordingly, these subtypes have been chosen for radiotracer development[6, 96, 97]. However, these nAChRs are not only key proteins in neurodegenerative diseases (Fig. 2A) but also in many other brain diseases such as drug addiction, schizophrenia (Fig. 2B), and possibly cancer (Fig. 2C). This offers the advantage that corresponding radiotracers may also be used to answer questions related to these diseases.

The radiotracer (*S*)-[^{11}C]nicotine, one of the very first positron-emitting receptor ligands, was initially developed to investigate the distribution of nicotine *in vivo* and later tested for PET imaging of nAChRs in the human brain[6, 98]. However, co-administration of unlabeled nicotine failed to displace much of the radioligand, indicating that the PET signal did not sensitively reveal specific binding to nAChRs. Cerebral (*S*)-[^{11}C]nicotine uptake proved mainly to be determined by blood flow, rather than the local abundance of nAChRs *in vivo*[6]. This indicates the importance not only of target but also of lead structure identification. Clearly, nicotine failed for the purpose of nAChR imaging. The discovery of various nAChR subtypes during the last two decades and their investigation have revealed different distributions and functions in various brain regions[6, 99]. Accordingly, different lead structures are needed to image them separately.

The selection process for development of ^{18}F-labeled radiotracers resembles the strategy used by the pharmaceutical industry in drug discovery. Although some features of radiotracers and drugs are different, the principal need remains: specific target binding. As discussed below, some selection criteria, such as affinity, selectivity, kinetic behavior, and metabolism may be even stronger for radiotracers than for common drugs. On the other side, characteristics like bioavailability, side-effects, and pharmacological efficacy are negligible. Regardless of the differences, the lead structures of pharmaceutical interest are usually the basis for radiopharmaceutical development.

Target Characterization and *in vitro* Screening of New Compounds

High-affinity binding is one of the most important prerequisites for radiotracers targeting neuroreceptors[100, 101]. As

a rule of thumb, a binding potential (BP = B_{max}/K_D) of >2 is required for a good PET radioligand[102]. This implies the need to search for higher target affinity ($1/K_D$) if the receptor density (B_{max}) is low. For example, the receptor densities for α7 nAChRs in the human brain are between 2 and 16 fmol/mg tissue[96]. Accordingly, a K_D between 1 and 8 nmol/L is required to fulfil the minimal criteria. The best α7 nAChR PET radiotracers available so far have affinities between 0.3 and 10 nmol/L[6].

Other important prerequisites for PET radiotracers are target selectivity and low non-specific binding[100, 101]. The displacement of radiotracer binding by ligands specific for non-target sites indicates lack of selectivity. This is a general disadvantage, because the specific signal obtained in neuroimaging studies is reduced (i.e. constitutes only a fraction of the total signal) in the presence of binding to non-target sites[100]. nAChRs, for example, comprise many subtypes expressed by at least 16 different genes[6, 103]. Many of them share a high degree of sequence identity and similarity with other nAChRs and also with other ligand-

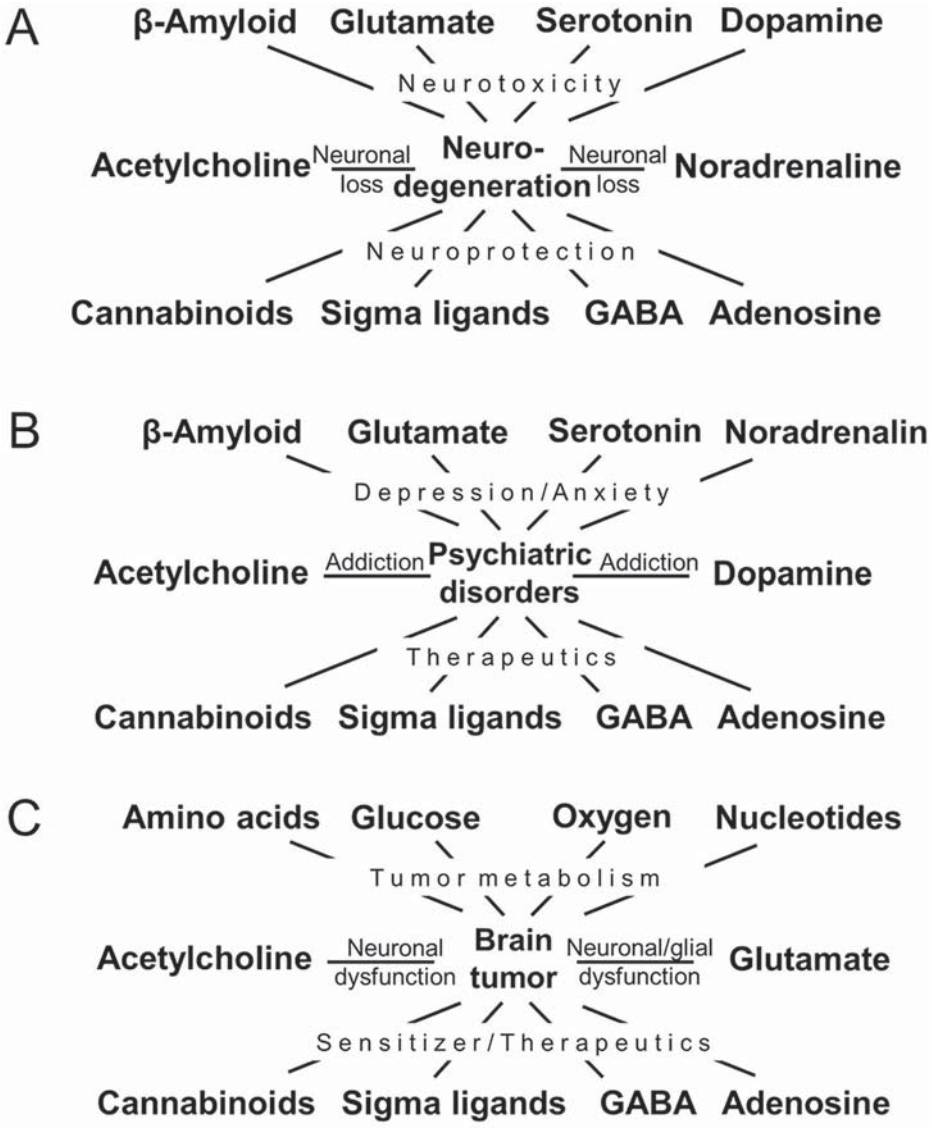

Fig. 2. Key molecules for development of new PET radiotracers for neuroimaging neurodegeneration (A), psychiatric disorders (B), and brain tumors (C).

gated ion channels[104]. Therefore, detailed investigation of non-target sites is important for the development of PET radiotracers for neuroimaging of nAChRs. In some cases, it is not the sequence-similarity of target proteins that is responsible for cross-reactivity but the chosen lead structure. A well-known example is vesamicol, which is the only known lead structure for targeting the vesicular acetylcholine transporter (VAChT). It has only a ten-fold higher affinity for VAChT than for σ receptors in the brain[105]. Improving this selectivity is still a challenge in the development of PET radiotracers for the VAChT[106].

The receptor densities and affinities of the respective ligands in target tissues are parameters that can be quantified *in vivo* by molecular imaging with PET. They are important during radiotracer development. To obtain such information, *in vitro* radioligand-binding assays can be used[100, 101]. The total binding measured in these assays is always a sum of target-specific binding, which has limited capacity and is saturable, and non-specific binding, which has a high capacity and is non-saturable at pharmacologically meaningful concentrations[100].

Given that the receptor density is determined by the target, higher BP values can only be achieved by higher ligand affinity. The binding affinity *in vitro* and *in vivo* may differ considerably because of the presence of different affinity states and other confounding factors[107]. Therefore, *in vitro* binding assays are the methods of choice to experimentally determine the affinity of new ligands. In particular, homogenate-binding or cell-binding assays allow high-throughput screening if needed. Alternatively, autoradiography on brain slices may be used; this is much more time-consuming but allows additional investigation of the regional distribution of receptors in the brain[100, 108].

With regard to nAChRs, the α4β2 subunit distribution has been investigated by *in vitro* autoradiography using [^{3}H]cytisine[109, 110] while the α7 nAChR has been characterized using [^{125}I]α-bungarotoxin[111, 112] or [^{3}H]methyllycaconitine[113]. For various reasons, these three ligands are not suitable as lead compounds for PET radiotracer development[6]. However, these highly selective compounds can be used to obtain information on the specific receptor binding of new drugs. For example, the highly-selective α7 nAChR ligand NS10743[114] (for structure see Fig. 7) is able to displace the binding of [^{125}I]α-bungarotoxin in the mouse brain (Fig. 3).

Concerning the α4β2 nAChR subtype, epibatidine has been used successfully as a lead compound since it has long been known for its high affinity for heteromeric nAChRs[115]. However, it has rather high toxicity arising from its potency and capacity to activate many different neuronal nAChR subtypes[116].

In order to improve the subtype selectivity, the fluoro-for-chloro-substituted homoepibatidine analogue, flubatine (previously called NCFHEB), has been synthesized[117] (Fig. 4). Results from [^{3}H]epibatidine binding assays performed with HEK293 cells expressing the human α4β2 nAChR (Fig. 5) show that both enantiomers of flubatine have affinities comparable to that of epibatidine and that the (+)-enantiomer has two-fold higher affinity than the other stereoisomer[117].

As expected from previous studies with fluoro- and norchloro-analogues of epibatidine[116], the newly-designed homoepibatidine analogues have 20- to 60-fold lower

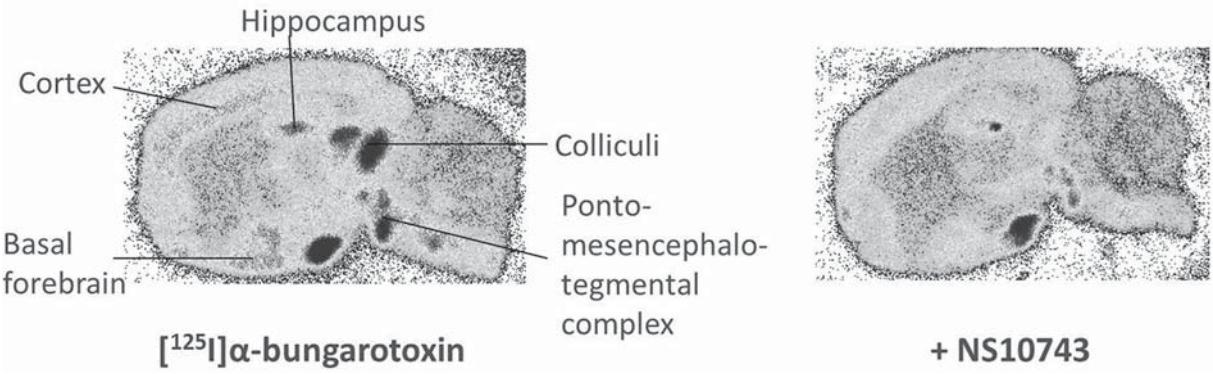

Fig. 3. NS10743, a lead compound for α7 nAChRs, displaces *in vitro* binding of the highly-selective [^{125}I]α-bungarotoxin in mouse brain.

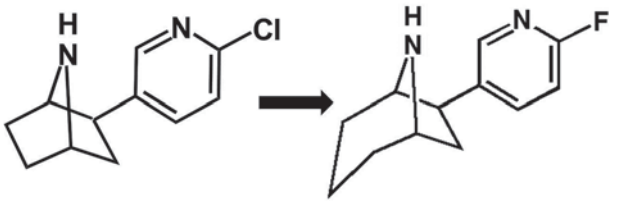

Fig. 4. Toxic epibatidine (left) and its less toxic derivative norchloro-fluoro-homoepibatidine (flubatine, right).

affinities to ganglionic α3β4 nAChRs than to the α4β2 subtype[117]. For flubatine, the increase in subtype selectivity seemingly results in decreased pharmacological side-effects compared to epibatidine. Intraperitoneal injection of 25 μg/kg (+)-flubatine or (–)-flubatine into awake mice is without important pharmacological effects[118]. Extended single-dose toxicity studies in rodents have shown a NOEL (No Observed Effect Level) of 6.2 μg/kg for (–)-flubatine

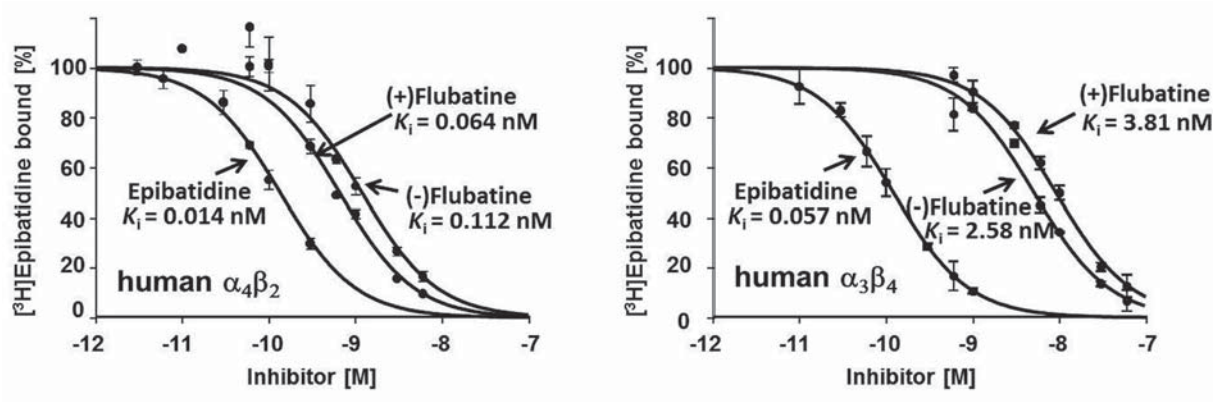

Fig. 5. Competition binding assays of [^{3}H]epibatidine on mem-branes prepared from cultured HEK293 cells stably transfected with α4β2 and HEK293 α3β4 cells. Increasing concentrations of epibatidine or flubatine were used for competition. Non-specific binding was determined in the presence of 300 μmol/L (–)-nicotine tartrate and subtracted from the total binding (adapted from Deuther-Conrad *et al.* Farmaco 2004[117]).

and 1.55 μg/kg for (+)-flubatine after i.v. injection[119]. These values are about ten-fold higher than those reported for *N*-methylepibatidine[120] and fluoro-norchloroepibatidine[121].

Regarding α7 nAChRs, many drug companies are developing receptor agonists and/or positive allosteric modulators for the treatment of schizophrenia and dementia[97]. Recently, NS10743, developed by Neuro-Search A/S (Ballerup, Denmark), has been characterized as a lead structure for PET radiotracer development. [^{3}H]Epibatidine-binding studies performed with HEK293 cells expressing the human α7, α3β4, or α4β2 nAChR have revealed K_i-values of NS10743 of 12 nmol/L, 84 nmol/L, and >10 μmol/L, respectively[114]. Together with autoradiographic evidence of specific receptor binding as shown in Fig. 3, these data encouraged the radiolabeling of NS10743 to obtain an α7 nAChR-selective PET radiotracer[114].

Occasionally, there is a lack of specific drugs that interact with certain brain proteins. For example, only a single lead compound AH5183, later called vesamicol[122, 123], has been identified for the VAChT so far. Accordingly, all the PET radioligands that have been developed for neuroimaging the VAChT are derivatives of this lead structure[106]. Major drawbacks of vesamicol are the relatively low affinity (K_i >10 nmol/L) and lack of selectivity. It binds to σ receptors with only ten-fold lower affinity[105] as well as to a "vesamicol-binding-protein"[124]. Similar affinity and selectivity have been found for (–)-FEOBV[125], a radioligand first described in 1993[126] and recently chosen for human VAChT studies[127]. Autoradiographic investigations of the human brain have revealed that [^{18}F]FEOBV binding is decreased by 33% in the prefrontal cortex, 25% in hippocampal CA3, and 20% in the CA1 region of patients with AD[128]. Although this was interpreted as cholinergic depletion, reduced σ_1 receptor binding cannot be excluded, because a 26% loss of this receptor has also been described in the CA1 region of patients with AD[90]. So far, no ideal PET radiotracer for the VAChT has been developed[106] and optimization of the binding affinity

of vesamicol-type ligands has been hampered by the lack of respective quantitative structure-activity relationships. Therefore, molecular modeling approaches have been used to predict the binding affinity of vesamicol-type/like ligands for VAChT from their molecular structures[125, 129].

A completely different situation is found with regard to radiotracer development for σ_1 receptor imaging. These receptors have an unusual multi-drug binding spectrum and the respective ligands cover diverse structural classes[89]. Therefore, selectivity not only for the other subtype (σ_2 receptor) but also for a great variety of further potential binding sites needs to be considered. Choosing spiropiperidines as lead structures, which fulfill these criteria and display a lack of significant binding to a great variety of different targets[130-132], has enabled successful PET radiotracer development[89]. However, structural modification was needed to introduce fluorine in a suitable labeling position. Accordingly, various series of derivatives have been synthetized to select those with the highest affinity, selectivity, and *in vitro* metabolic stability[133-138]. Very high selectivity towards the VAChT has been found, excluding cross-reactions with this target[139].

Physicochemical Characterization of Lead Compounds

Besides affinity and selectivity, some basic physicochemical properties of the parent compound have to be considered before radiolabeling. Lipophilicity, measured for example as log*P* and/or log*D* in octanol/water partition experiments, and molecular weight are important determinants for the compound´s ability to cross the BBB[140, 141]. Small-molecule drugs may sufficiently cross the BBB *via* lipid-mediated free diffusion if they have a molecular weight <400 g/mol and form <8 hydrogen bonds[141]. However, the majority of small-molecule drugs and all large-molecule drugs lack these chemical properties[141]. Considering these limitations, increasing lipophilicity may enhance the BBB permeability, but it also tends to increase plasma protein binding, causing a decrease of drug availability. Consequently, a parabolic relationship exists between lipophilicity and BBB permeability[107]. For a series of benzamides targeting the dopamine D_2 receptor, an optimal log*P* between 2 and 3 has been determined[142]. Accordingly, there is a rather small window of appropriate combinations of lipophilicity, molecular weight, and affinity. Nevertheless, a nearly infinite number of substances can theoretically be synthesized from basic organic elements within the restraints described above.

Significant deviations from the above parabolic relationship have been found, which can be ascribed to the existence of multiple mechanisms of drug transport through the BBB[143]. There is clear evidence that the expression of active efflux pumps like the multidrug transporter P-glycoprotein (P-gP) at the BBB accounts for the poor permeability of certain drugs (see below). Undoubtedly, P-gP is an important barrier to the entry of hydrophobic drugs into the brain[144]. Thus, proper prediction needs to consider active transport phenomena.

Furthermore, a variety of nutrient transporters expressed at the BBB are able to transport certain xenobiotics and drugs[141, 143]. Recently, it has been shown that the α4β2 nAChR PET radiotracer [^{18}F]flubatine (formerly called [^{18}F]NCFHEB) interacts with carrier-mediated choline transport at the BBB[118].

Preparation of Labeling Precursors and Radiolabeling

Considering the short half-lives of the radionuclides used for radiolabeling (e.g., 20.4 min for ^{11}C and 109.8 min for ^{18}F) they need to be incorporated into appropriate precursor molecules quickly. Ideally, the precursor molecules should allow rapid labeling in a maximum of two synthetic steps. As a rule of thumb, the whole labeling procedure including purification and formulation of the final product, should not last longer than two to three half-lives (for ^{11}C). Accordingly, labeling precursors are not necessarily chemically similar to the respective radiolabeled compound/non-radiolabeled reference compound.

Furthermore the precursor should allow (1) high reproducibility of the reaction, (2) automation of the production process (labeling, purification, formulation), and (3) accomplishment of an absolute radiochemical yield (RCY) of the formulated product high enough to permit human application. Ideally, the latter should enable routine as well as commercial production of the radiopharmaceutical.

Fluorine forms very strong covalent C-F bonds that provide valuable chemical, physical, and biological properties to organic molecules that contain one or more

fluorine atoms attached to aromatic carbon. However, because of the reactivity and hazards of elemental fluorine and hydrogen fluoride, the task of introducing fluorine into organic molecules has been a particular challenge to synthetic chemists and has led to the development of specialized fluorination techniques and reagents[145, 146].

Generally, fluorine can be introduced into organic molecules by electrophilic fluorination reactions using elemental fluorine or by nucleophilic fluorination using inorganic and other ionic fluorides. Although various fluorinating agents have been reported in organic fluorination reactions, only two agents are suitable for direct radiofluorination reactions with ^{18}F: [^{18}F]F_2 and its derivatives (such as [^{18}F]acetylhypofluorite for electrophilic fluorination and [^{18}F]fluoride for nucleophilic substitutions[147-149]). For regioselective introduction of ^{18}F, activated precursor molecules like trialkylstannyl-substituted arenes are needed.

Electrophilic fluorination is quite fast and efficient, making it a highly desirable synthetic method to obtain metabolic radiopharmaceuticals such as the glucose derivative [^{18}F]FDG (*via* the old-fashioned synthetic pathway using glycals) or the amino acid [^{18}F]FDOPA. Unfortunately, the products suffer from low specific activity owing to the carrier-added non-radioactive fluorine[147, 148] and thus are excluded from use for neuroreceptor imaging.

The only exception is the post-target-produced highly specific [^{18}F]F_2 of up to 55 GBq/μmol[150] and its use for [^{18}F]CFT synthesis, a dopamine transporter ligand[151]. Therefore, no further attention is given to electrophilic radiofluorination in this review. Furthermore, special methods for ^{18}F-labeling of peptides and proteins are not considered, because these molecules are not suitable for brain imaging due to their very low BBB transport rates[152].

Nucleophilic substitution primarily depends on the activation of the [^{18}F]fluoride ion ([^{18}F]F^-) – so-called “naked fluoride” – starting from irradiated ^{18}O-enriched target water. This is reached by the generation of ion pairs consisting of bulky counter-ions for the [^{18}F]F^- such as K^+-chelating agents or tetraalkylammonium ions[153, 154].

In the presence of aprotic or very weakly-acidic protic solvents, the counter-ion/[^{18}F]F^- - ion pair is available as a highly reactive nucleophile. In combination with suitable precursors provided with properly reactive leaving groups, nucleophilic substitution reactions may occur.

Nucleophilic substitution depends on properly active leaving groups for the ^{18}F-fluoride exchange reaction. Its selection depends on various chemical properties of the compounds to be labeled. For radiosynthesis of a desired ^{18}F-labeled compound *via* nucleophilic substitution, a distinction generally has to be made between aliphatic and aromatic procedures.

For aliphatic nucleophilic substitutions[155], in most cases, the anions of sulfonic acids such as triflate, tosylate, mesylate, or nosylate groups are the preferred leaving groups. An option to introduce ^{18}F to aliphatic (or even deactivated aromatic) moieties of a molecule is the use of its halide derivatives. The approximate order of increasing suitability for aliphatic reactions is: I > Br > Cl > F, which is the reverse of that found in aromatic nucleophilic substitution reactions[156]. In the radiolabeling of various fluoro-alkyl indiplon derivatives, the use of bromine as the leaving group has an RCY (38-43%) similar to the use of a tosylate leaving group[157-159]. Notably, depending on the length of the alkyl chain, *O*-tosyl-containing precursor molecules gradually decompose over months[159]. Using a halide leaving group, even isotopic ^{19}F (stable fluorine) for ^{18}F exchange with minor precursor amounts is an option[160]. Ring opening of cyclic reactive entities offers another method for the introduction of radiofluorine[161].

Fluoro-aromatic compounds are known to be extraordinarily stable. This is true for the C-F bond too. Accordingly, radiofluorinated derivatives are very suitable radiotracers. For their no-carrier-added radiosynthesis, aromatic nucleophilic substitutions on deactivated (electron-deficient) aromatic ring systems (i.e. activated in terms of nucleophilic reactions) with suitable leaving groups are needed. This activation is caused by electron withdrawing groups, whereas trialkylammonium (-$N(Me_3)^+$) or nitro groups or special combinations of both act as leaving groups[162]. For aromatic nucleophilic substitution reactions, the -$N(Me_3)^+$ group is preferred because it usually allows more reproducible radiosynthesis with higher RCYs. Beside deactivated carbocyclic aromates, pyridine rings are a valuable tool to be radiofluorinated as they are already deactivated moieties. Recently, seven different strategies for radiolabeling the α4β2 nAChR ligands (–)/(+)-[^{18}F]flubatine were compared[163]. The original radiosynthesis using a bromo-pyridine precursor and an ethoxycarbonyl protecting group at the tropane

nitrogen requires a microwave reaction followed by chiral HPLC separation of the enantiomers and provides overall RCYs of only 2%, which is insufficient for routine clinical PET investigation[164]. Several variations of leaving groups coupled in the ortho-position to pyridine nitrogen (-Cl, -NO_2, -$N(Me_3)^+$/iodide, -$N(Me_3)^+$/triflate) and protecting groups (-Boc, -Trityl, -Fmoc) have been investigated. The use of chlorine was unsuccessful, while the use of –NO_2 revealed ~75% lower labeling efficiency than that of -$N(Me_3)^+$/iodide or -$N(Me_3)^+$/triflate. A combination of the $N(Me_3)^+$/iodide precursor and a Boc-protecting group provided the best results with an RCY of 60 ± 5%[163]. The radiosynthesis was independent of the use of a microwave and was easily transferable to automated synthesis modules to prepare for human application. Recently, automated synthesis has been reported by two institutions with RCYs of 30%[165] and 25%[166].

The above-mentioned electron withdrawing groups (-I effect, -M effect) bound to aromatic moieties are a definite need to enable a nucleophilic attack. In a recent study on radiolabeling of cannabinoid receptor type 2-selective compounds (Fig. 6), the summarized effect of bromine in the *meta*-position to the leaving group –NO_2 was regarded to be not strong enough to achieve an RCY >3%[167]. An introduction of nitrogen into the aromatic ring facilitated the nucleophilic substitution (RCY >28%) but reduced the affinity by a factor of 30[167]. To retain the affinity (K_i = 4.3 nmol/L), a –$N(Me_3)^+$ precursor was synthesized and used for radiolabeling and provided RCYs between 30% and 35%[168].

Besides low labeling yields, the use of bromine precursors may have further disadvantages such as an unsatisfactory quantitative separation of the radiolabeled product and its precursor (Fig. 7). Initial attempts to use a bromine precursor for radiolabeling of NS10743, a highly selective α7 nAChR ligand, failed.

For some molecules, the structure does not allow nucleophilic substitution or the radiotracers decompose under the accompanying harsh conditions. In these cases, labeling can be achieved by a multistep procedure using small generic groups that allow both derivatisation with fluorine as well as convenient introduction of radiofluorine. These groups are referred to as secondary labeling precursors or prosthetic groups[148, 169, 170]. A large number of these ^{18}F-labeled intermediates have been prepared and investigated, such as amines, alcohols, aldehydes, ketones, carboxylic acids, esters, and halides[148]. In particular, [^{18}F]fluoroalkynes and [^{18}F]fluoroalkylazides are interesting prosthetic groups as they can be coupled to a variety of molecules using the Huisgen “click” reaction which proceeds in high RCYs in aqueous solution under mild conditions. Thus, it can be used for the radiolabeling of water-soluble biomolecules[148, 171-175]. Generally, careful selection of prosthetic groups is critical for radiotracer development as they often exert great influence on target binding and/or *in vivo* stability[169].

A further path to ^{18}F-labeled radiotracers is starting the labeling of a pre-prepared substance (reactive precursor) in a first step and its chemical transformation in a subsequent reaction into the final product. This is demonstrated by means of a ring closure reaction (McMurry coupling, Fig. 8).

We have recently used ^{18}F-labeled alkyltosylates for the radiolabeling of phenolic precursors *via* etherification to obtain high-affinity and selective radiotracers for the serotonin transporter[177] and the enzyme phosphodiesterase 10A[178], respectively, with RCYs between 11% and 25%. High metabolic stability of the ether bond is expected because negligible defluorination was observed[178].

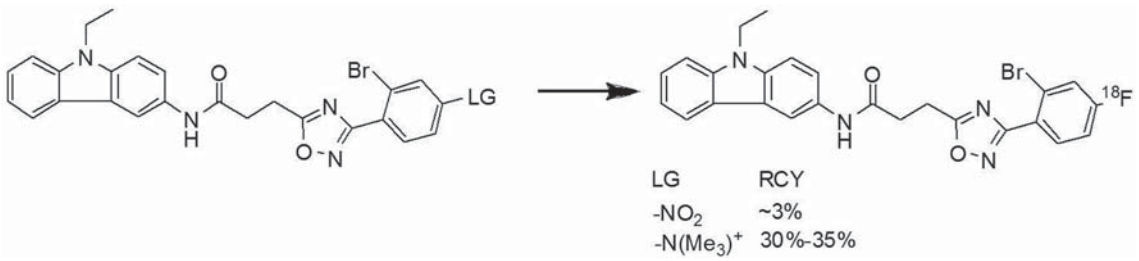

Fig. 6. Effect of leaving group (LG) on radiolabeling yield of a new cannabinoid receptor type 2-selective drug. RCY, radiochemical yield.

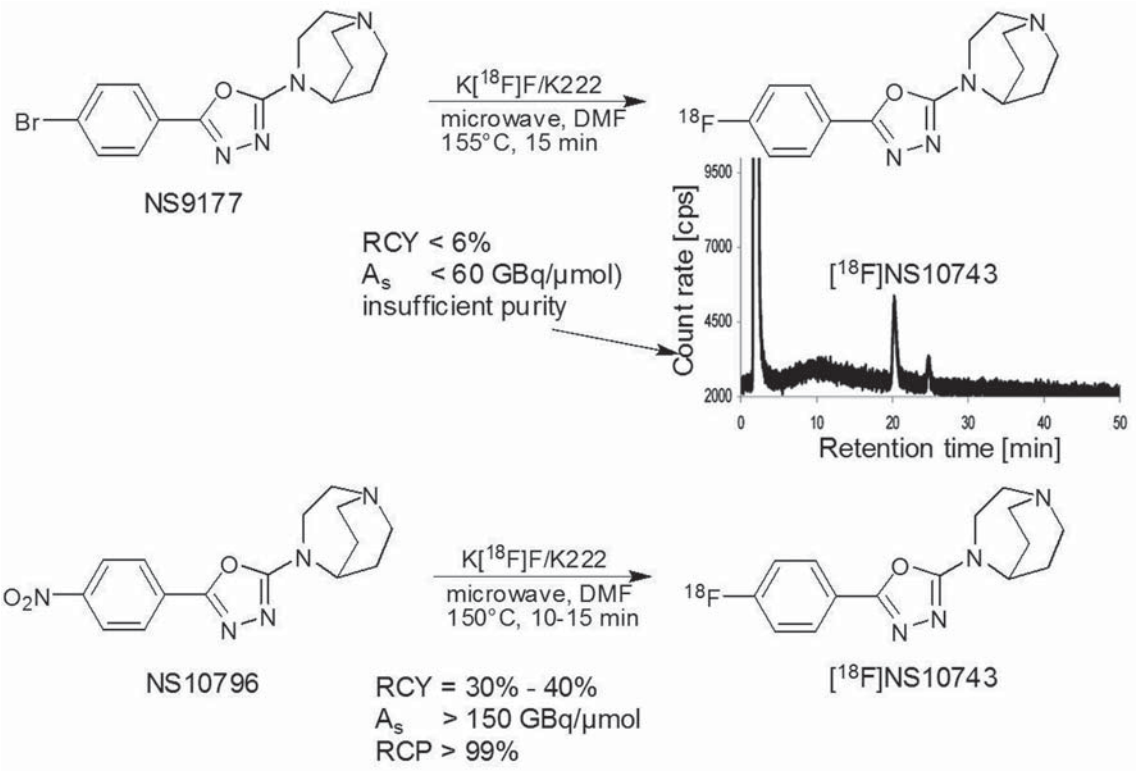

Fig. 7. Radiosynthesis of the α7 nAChR ligand [^{18}F]NS10743 using two different precursors. The bromo precursor NS9177 proved unsuitable for radiolabeling. The radio-HPLC sample is from the reaction mixture with the bromo precursor. RCY, radiochemical yield.

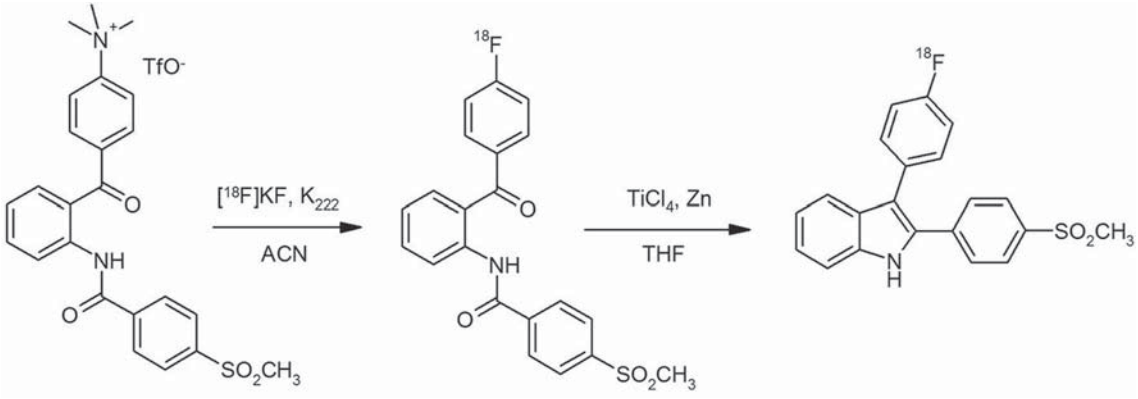

Fig. 8. Introduction of [^{18}F]fluoride into a complex molecule in a first step and subsequent McMurry coupling to the final product, a PET-tracer for imaging cyclooxygenase-2[176].

By contrast, [^{18}F]fluoroacetamides have proven to be metabolically unstable due to hydrolytic cleavage[169]. Thus, high-affinity and selective radiotracers for the VAChT[179] and the $GABA_A$ receptor[180], respectively, are not suitable for *in vivo* imaging because metabolites that cross the BBB are generated. The metabolic instability is caused by the action of hydrolytic enzymes, e.g. carboxylesterase[169]. In such cases, the use of [^{18}F]fluoropropane sulfonamides

can be recommended because of their stability against carboxylesterase-mediated hydrolysis[169].

Specific Binding of Radiotracers *in vitro*

To determine the specific target binding of newly-developed radiotracers, various *in vitro* binding assays can be used[100]. These provide specific features useful for target characterization and *in vitro* screening; an example of affinity determination of [^{18}F]NS10743[114] is shown in Fig. 9. In a homologous competitive binding assay using SHSY5Y cells expressing the human α7 nAChR and increasing concentrations of [^{18}F]NS10743 as radiotracer, an equilibrium dissociation constant K_D of ~9 nmol/L was estimated. Non-specific binding was determined in the presence of 300 μmol/L (−)-nicotine tartrate and subtracted from the total binding.

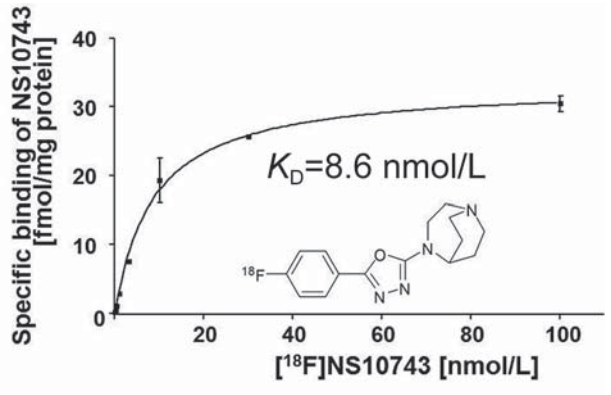

Fig. 9. Saturation analysis of [^{18}F]NS10743 binding on membranes prepared from cultured SHSY5Y cells expressing the human α7 nAChR. Non-specific binding was determined in the presence of 300 μmol/L (–)-nicotine tartrate and subtracted from total binding.

Alternatively, *in vitro* binding affinity can also be determined by autoradiography, where brain slices are incubated with increasing radiotracer concentrations. Although more time-consuming, this technology has the advantage that additional information on the regional distribution of the target within the brain is available. As an example, Fig. 10 shows the distribution of α4β2 nAChRs in rat brain as determined with the two enantiomers of [^{18}F]flubatine. Brain slices were incubated with increasing radiotracer concentrations to obtain data on target density and radiotracer affinity. As expected, these clearly show the highest receptor densities in the thalamus, superior colliculus, and nucleus interpeduncularis[181]. Unexpectedly, different affinities were estimated for the various regions. In principle, this may be caused (1) by a remaining part of the endogenous ligand (ACh) competing with the radiotracers, (2) different allosteric receptor regulation in the various regions, or (3) by additional binding to (an)other target(s).

In another experiment (Fig. 11), additional information was obtained on the selectivity of (–)-[^{18}F]flubatine for α4β2

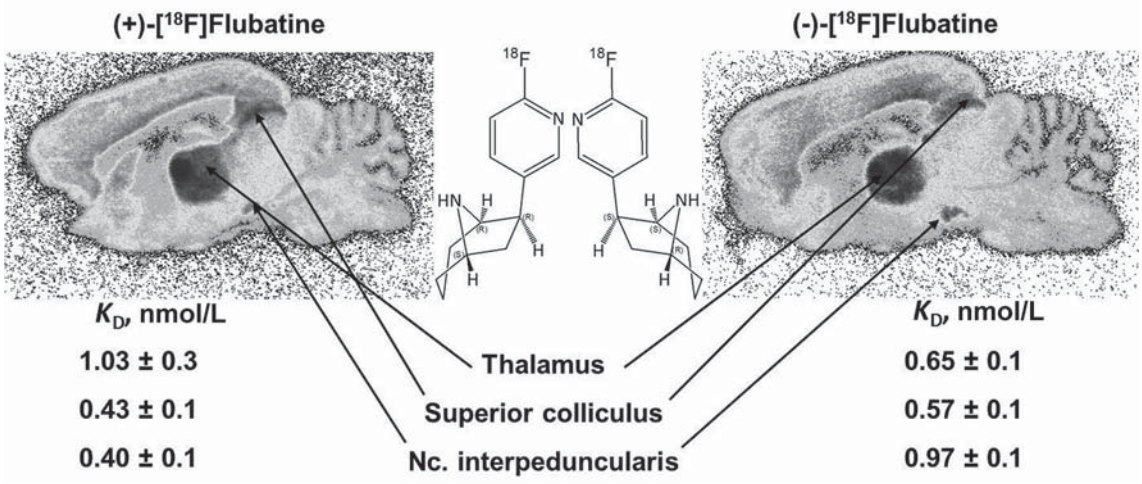

Fig. 10. *In vitro* autoradiographs of α4β2 nAChR distribution in rat brain using (+)-[^{18}F]flubatine and (–)-[^{18}F]flubatine as radioligands. Increasing concentrations of flubatine were used for homologous competition. Non-linear regression analysis was used to estimate the affinities ($1/K_D$) in various brain regions. Nc, nucleus.

nAChRs. The radiotracer binding in pig brain was inhibited by co-incubation with various drugs of different selectivities for nAChRs. The nonselective inhibitor epibatidine[182] and the β2-subtype-selective inhibitors A-85380[183] and cytisine[182] clearly reduced the (–)-[^{18}F]flubatine binding, whereas the α7-subtype-selective inhibitor MLA[184] did not.

Furthermore, autoradiographic experiments are well-suited to compare various radiotracers and target binding in different species. For example, the distribution of $GABA_A$ receptors in pig brain as measured with the gold-standard [^{3}H]flunitrazepam and a new ^{18}F-labeled indiplon[185] derivative[186] is similar to that in rat brain (Fig. 12). Another example shows the use of [^{3}H]citalopram, the most selective serotonin transporter radioligand[187], to obtain *in vitro* autoradiographs of serotonin transporter (SERT) distribution in the pig brain (Fig. 13). Cresyl violet staining of parallel slices allowed the precise delineation of numerous brain regions and correlation analysis between autoradiographs of the gold-standard ([^{3}H]citalopram) and a new PET radiotracer ([^{18}F]FMe-McN5652). A highly significant correlation between the radioligands (r = 0.9, P < 0.001) was found[188].

Usually, *in vitro* autoradiography is a good predictor of the imaging properties of a new radiotracer. However, radiotracers with unacceptable *in vitro* data are still able to provide good images *in vivo*. An example is the dopamine transporter-selective SPECT radiotracer [^{99m}Tc]TRODAT-1. *In vitro* autoradiography with this radiotracer shows a high non-specific background with less conspicuous binding in the rat striatum, a dopamine-transporter-rich brain region[189]. Meanwhile, [^{99m}Tc]TRODAT-1 has been introduced into the clinic as a tool for the diagnosis of Parkinson's disease[190].

Metabolism of Radiotracers in Animals

Investigation of radiotracer metabolism *in vivo* needs special consideration, especially for neuroimaging. Because of the exceptionally great functional diversity of the brain compared to other organs, there is a need to precisely differentiate between various brain regions with

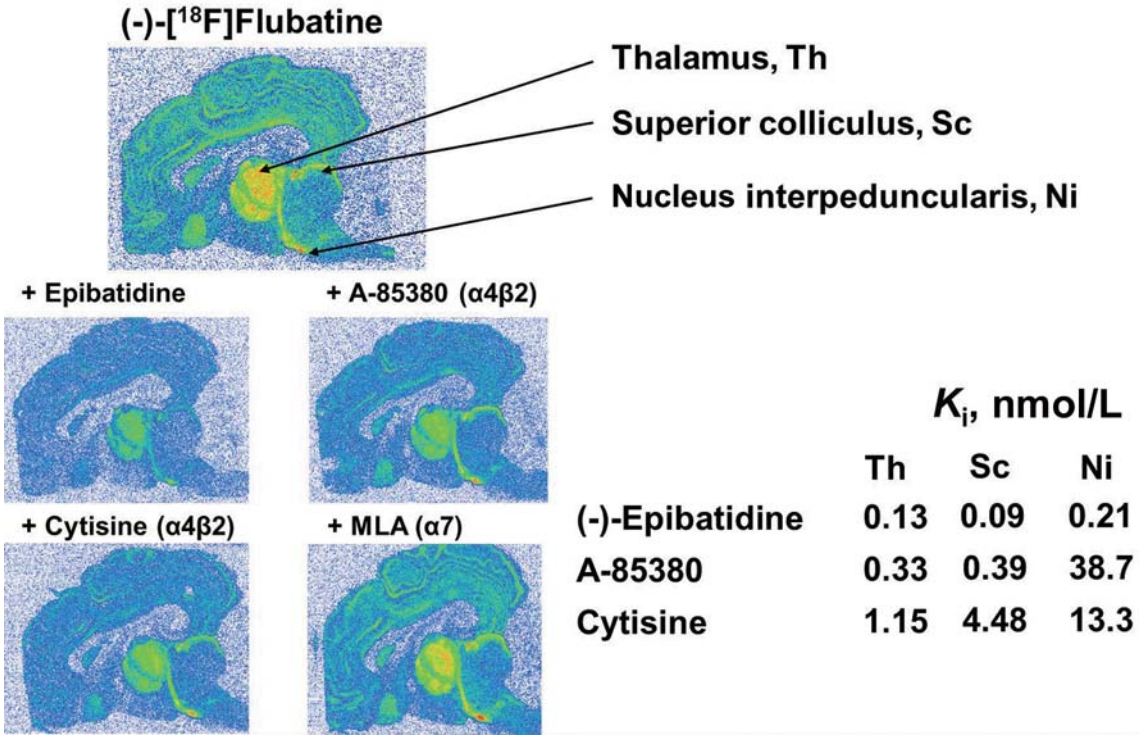

Fig. 11. ***In vitro*** **autoradiographs of α4β2 nAChR distribution in pig brain using (–)-[^{18}F]flubatine as radioligand. Epibatidine, A-85380, cytisine and MLA were used as competitors to assess the specificity and selectivity of radiotracer binding to α4β2 nAChRs.**

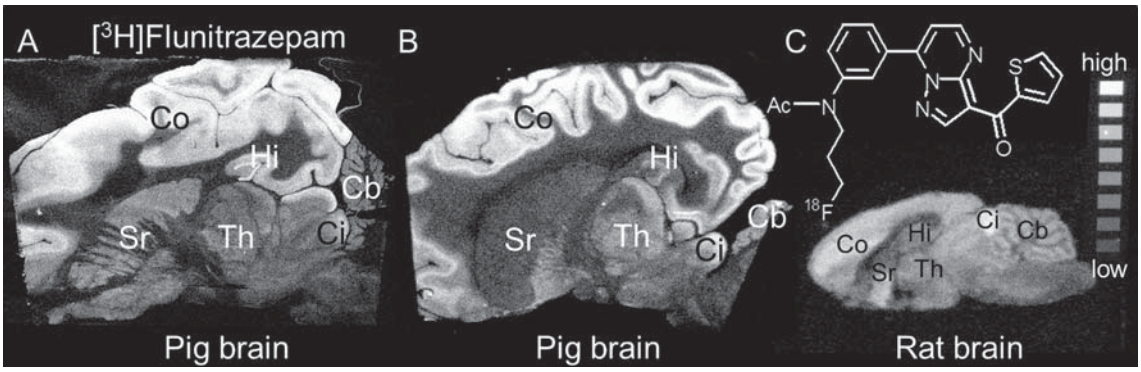

Fig. 12. ***In vitro*** **autoradiographs of GABA$_A$ receptor distribution in pig and rat brain using [^{3}H]flunitrazepam and a new ^{18}F-labeled indiplon derivative[186] as radioligands (adapted from Deuther-Conrad *et al.* Curr Radiopharm 2009[158]).**

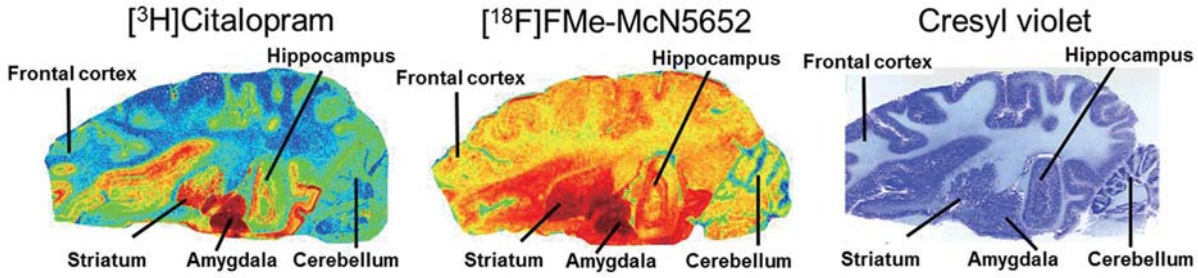

Fig. 13. ***In vitro*** **autoradiographs of serotonin transporter distribution in pig brain using [^{3}H]citalopram and [^{18}F]FMe-McN5652 as radioligands, compared to an adjacent cresyl violet-stained brain slice (adapted from Kretzschmar *et al.* Eur Neuropsychopharmacol 2003[188]).**

regard to specific radiotracer binding and target density. Therefore, it has to be ensured that the PET image is derived from the radiotracer only and not blurred by the presence of radiolabeled metabolites. Consequently, the potential presence of radiometabolites in the brain needs to be investigated and ideally excluded. Furthermore, the use of compartmental models for the quantitation of receptor binding parameters depends on an exact measurement of the radiotracer availability for brain uptake. Accordingly, the radioactivity measured in blood samples needs to be corrected by subtraction of the amount of radiometabolites.

Standard chromatographic methods such as high-performance liquid chromatography (HPLC), thin-layer chromatography (TLC) and solid-phase extraction (SPE) are used to separate the radiotracer and its metabolites. In principle, all methods are based on the different interactions of various analytes with the stationary and mobile phases. After separation has been achieved, the activity of the analytes is determined by special online activity detectors integrated into the HPLC system, by autoradiography of TLC plates, or by measurement of eluted substances in well-counters. While HPLC and TLC are standard procedures during radiotracer development, SPE offers advantages in the clinical setting because of its high throughput and low cost. However, SPE has to be validated by comparison with HPLC or TLC before use.

A common concern in the development of PET radiotracers for neuroimaging is the presence of lipophilic metabolites in blood, because they are likely to cross the BBB just because of their lipophilicity[107]. Such metabolites may either be active, i.e. having a target-affinity high enough for significant binding, or inactive. In the former case, quantification is highly confounded because the measured signal represents undetermined proportions of parent tracer and metabolite, each of which may have a different affinity for the target[107]. In the latter case, non-

specific binding is increased, leading to a decreased signal-to-noise ratio.

For example, the 5-HT_{2A} receptor PET radiotracer [^{18}F]altanserin is metabolized by reduction of ketone to yield [^{18}F]altanserinol, which is transported across the BBB[191]. In the brain, it contributes to non-specific binding. However, the signal obtained from specific receptor binding is regarded to be unchanged because the affinity of altanserinol for serotonin receptors is negligible[191]. This offers the possibility of using [^{18}F]altanserin together with a constant infusion paradigm for quantification of 5-HT_{2A} receptor availability in the brain[191, 192]. Alternatively, the use of the simplified reference tissue model (see below) allows consideration of the presence of radiometabolites in brain, as long as their contribution to non-specific binding is homogenous throughout and there is a reference region without specific binding[193].

Confounding effects of brain metabolites on dopamine transporter (DAT) imaging have been observed for a variety of radiotracers such as [^{123}I]β-CIT[194], [^{11}C]β-CIT[195], [^{18}F]FECNT[196], [^{11}C]PE2I[197], and [^{11}C]/[^{18}F]LBT-999[198].

In the case of β-CIT, lipophilic metabolites have been detected[194, 195]. Accordingly, labeling of β-CIT with ^{11}C by either *N*-methylation or *O*-methylation has resulted in radioligands with different kinetics in the monkey brain. Preparation of two of the putative labeled metabolites [*N*-methyl-^{11}C]β-CIT-acid and [*O*-methyl-^{11}C]nor-β-CIT, and investigation of their brain uptake, revealed that <0.4% of the injected [*N*-methyl-^{11}C]β-CIT-acid entered the brain whereas 5%–6% of the more lipophilic [*O*-methyl-^{11}C] nor-β-CIT entered and accumulated in the striatum and thalamus. Notably, nor-β-CIT has been found to specifically bind to the serotonin transporter[199], providing an additional confounding effect.

Regarding [^{11}C]PE2I, a benzyl alcohol metabolite derived from biotransformation by cytochrome P450 enzymes residing predominantly in the liver[200], has been shown to cross the BBB[197]. In the brain, it is supposed to be further metabolized by alcohol and aldehyde dehydrogenases. Also, for [^{11}C]LBT-999 and [^{18}F]LBT-999, hydroxylated derivatives have been found. Their accumulation in the striatum indicates specific binding to the DAT[198].

For [^{18}F]FECNT, *N*-dealkylation has been shown to provide a brain-penetrant radiometabolite of even higher *in vitro* DAT affinity than the parent compound itself, preventing the use of a reference tissue model for quantitation[196, 201].

Lipophilicity is not necessarily a prerequisite for brain uptake of radiometabolites. [^{18}F]fluoroacetamides have been shown to be metabolically unstable due to hydrolytic cleavage of the amide bond. The resulting highly hydrophilic [^{18}F]fluoroacetate is transported into the brain[202-204], at least partly mediated by carboxylic acid transporters at the BBB[205]. [^{18}F]fluoroacetate was proposed as a major metabolite of radiotracers for imaging the VAChT, e.g. [^{18}F]FAMV[179] and [^{18}F]FAA[206], or $GABA_A$ receptors[180], preventing the use of these radiotracers for neuroimaging. Interestingly, it was found that fluoroacetate is defluorinated by glutathione *S*-transferases[207] which are highly expressed in brain tissue[208]. To explain the high amounts of radioactivity in rat ventricles after injection of [^{18}F]FAMV, it was proposed that the elimination of brain metabolites may occur by clearance *via* the cerebrospinal fluid[179].

Besides knowledge regarding the potential of radiometabolites to cross the BBB, information on the precise amounts of radiometabolites in plasma is often needed for quantitation of receptor binding of PET radiotracers *in vivo* (see below). The faster the metabolism, the stronger the alterations of the input functions and the influence of potential bias. Determination of metabolites in rodents or larger animals such as pig or monkey provides suitable estimates for clinical PET studies. Because of the higher surface-to-volume ratio, the influence of metabolism on the PET quantitation of human data is usually overestimated when investigated in experimental animals. Thus, for the serotonin transporter PET radiotracers (+)-[^{11}C] McN5652 and [^{18}F]FMe-McN5652, the metabolism in pigs[209] is about twice as fast as measured in humans[210, 211]. Another very good example is the α4β2 nAChR PET radiotracer (–)-[^{18}F]flubatine. Rather strong differences between pigs and humans have been reported. While ~60% of metabolites were found in pig plasma at 2 h after injection[212], this value was only ~10%–15% in humans[213]. Because of this very low amount of radiolabeled metabolites, full kinetic modeling was possible even without metabolite correction of the input function[214], which is of great advantage for routine clinical use.

The high metabolic stability of flubatine has recently

been confirmed in an *in vitro* study comparing mouse and human microsomal preparations (containing enriched cytochrome P450 enzymes[215, 216]), where a 5–6-times faster metabolism was found in mice. Interestingly, the (–)-enantiomer is significantly less stable than the (+)-enantiomer (unpublished data). Stereoselective metabolism of drugs by P450 enzymes is a common phenomenon and may also explain differences in the metabolism of other enantiomeric PET radiotracers, such as (+)-/(–)-[^{11}C]McN5652[211] or the σ_1 receptor-selective (*R*)-/(*S*)-[^{18}F]fluspidine[136].

Proof of Target-specific Binding in Animals

Usually one of the first steps to demonstrate target-specific binding *in vivo* is the investigation of radiotracer biodistribution in mice or rats. Although *in vitro* studies allow the estimation of target affinities, the bioavailability of radiotracers is a confounding factor for target binding *in vivo*. The bioavailability of radiotracers is influenced by blood flow, plasma protein binding, membrane permeability, and metabolism. Furthermore, the optimized settings used for radioligand binding assays usually differ from the physiological conditions found *in vivo* where different pH and temperature as well as the presence of endogenous competitors may be confounding factors. The complex interaction of all these parameters can only be investigated *in vivo* and justifies the approval of animal experiments by legislative authorities.

Information on the time-dependent biodistribution of radiotracers can be obtained by *ex vivo* tissue sampling or small-animal imaging[7, 100]. The two methods are rather complementary than competitive, both offering advantages and disadvantages (see Table 2). More detailed information is available elsewhere[100].

In addition to the use of rodents for *ex vivo* tissue sampling or small-animal imaging, larger animals such as monkeys or pigs are used for PET imaging with human scanners.

Independent of the type of *in vivo* study chosen, the strategy to obtain certain information about the radiotracer is similar. Studies have to show that the brain uptake is sufficiently high, specific, and selective to justify human application for neuroimaging. Furthermore, data obtained on whole-body radiotracer kinetics can also be used to estimate the absorbed radiation dose as a prerequisite for human application[217].

The magnitude of brain uptake is mainly determined by the size, lipophilicity, and H-bonding capacity of the radiotracer[141, 218], i.e. parameters accessible by *in vitro* investigations. The brain uptake may occasionally be confounded by affinity for efflux transporters at the BBB. A variety of *in vitro* systems representing the BBB have been described, but the optimal use of these data, in terms of extrapolation to human unbound brain concentration profiles, remains to be fully exploited[219]. Therefore, animal experiments are still indispensable to investigate this aspect. Notably, the expression of the various efflux

Table 2. Advantages and limitations of *ex vivo* tissue sampling and small-animal imaging

Parameter	*Ex vivo* tissue sampling	Small-animal imaging
Anesthesia	Just before death	Throughout the study
Applied activity (per mass)	~ Human dosage	>> Human dosage
Radiation damage	Unlikely	Possible
Estimation of absorbed radiation dose	Possible	Possible (preferred)
Multiple time point measurements	Multiple subjects needed	Single subjects
Longitudinal studies	Not possible	Possible
Animal models of disease	Relatively high expenses	Possible
Tracer kinetic modeling	Relatively high expenses	Possible
Physiology	Unaffected	Potentially affected
Blocking effects of drugs	Unaffected by applied dosage	Potentially affected by applied dosage

transporters at the BBB differs significantly between species[220, 221]. Among drug transporters, breast cancer resistance protein appears to be most abundant with an expression level ~2-fold greater in humans than in mice. By contrast, the expression level of P-gP in humans is ~2.5-fold lower than the corresponding mdr1a gene in mice[221]. Consequently, low brain uptake in rodents does not necessarily forecast the uptake in other species like humans. For example, the brain uptake of the high-affinity and selective α7 nAChR ligand [^{18}F]NS14492 is ~10-times higher in pigs than in mice, suggesting suitability for human brain imaging[222]. Similar species differences between rats, guinea pigs, and monkeys have been reported for the 5-HT$_{2A}$ receptor ligand [^{18}F]altanserin, the NK1 receptor antagonist [^{11}C]GR205171, and the classical P-gP substrate [^{11}C]verapamil[223].

The specificity and selectivity of brain uptake is another important issue to consider in animal experiments[7]. For targets with a heterogeneous distribution, the ratio of brain uptake between a region with high target expression and a region with negligible or low target expression represents a reasonable measure of specific binding. A typical example is the dopamine D$_2$ receptor. The caudate/cerebellum ratio was used to verify specific binding of the first (D$_2$-receptor specific) PET radiotracers, 3-*N*-[^{11}C]methylspiperone and [^{11}C]raclopride, in human and monkey[224, 225]. Since these early studies, the cerebellum has often been used as suitable reference region for the development of PET radiotracers for other dopamine receptors[226], serotonin 5-HT$_{1A}$ and 5-HT$_2$ receptors[227, 228], muscarinic and nicotinic ACh receptors[229-231], histamine receptors[232], and the serotonin transporter[188, 233]. An example of *ex vivo* autoradiography of SERT distribution in rat brain where the radiotracer [^{18}F]FMe-McN5652 (30 MBq) was injected intravenously is shown in Fig. 14B. The animal was sacrificed 90 min later and the brain subjected to autoradiography. Regions with the highest SERT expression such as frontal cortex, striatum, and substantia nigra[187, 234] clearly showed the highest radiotracer accumulation, providing evidence for radiotracer selectivity[188]. Furthermore, comparison with an *in vitro* autoradiograph of rat brain (Fig. 14A) using the same radiotracer clearly showed a high correlation of SERT binding between the approaches.

An example of how an *ex vivo* binding ratio has been used to identify the radiotracer with the highest σ1 receptor binding in mouse brain among a series with various lengths of the alkyl side chain is shown in Fig. 15. Notably, for the σ$_1$ receptor, as for metabotropic glutamate receptor 1 (mGluR1)[59] and the GABA$_A$ receptor[180], the cerebellum is among the regions with the highest expression and cannot be used as a reference region in this case. The ratio between the region with lowest radiotracer accumulation (olfactory bulb) and that with highest accumulation (facial nucleus) was chosen for the estimation of specific receptor binding. Consistent with the highest brain-to-plasma ratio at 60 min post-injection and the highest target affinity, this ratio was highest for the ethyl derivative [^{18}F]fluspidine[89].

Besides the use of reference regions for the evaluation of specific receptor binding in brain, blocking studies are recommended. A high concentration of a drug that binds specifically to the receptor site is injected before or together with the radiotracer and thereby prevents its specific binding to the target[100]. From the difference between a control study and the blocking study, information on the specific binding can be obtained. Using a similar setup, the target selectivity of the radiotracer can be investigated. As shown

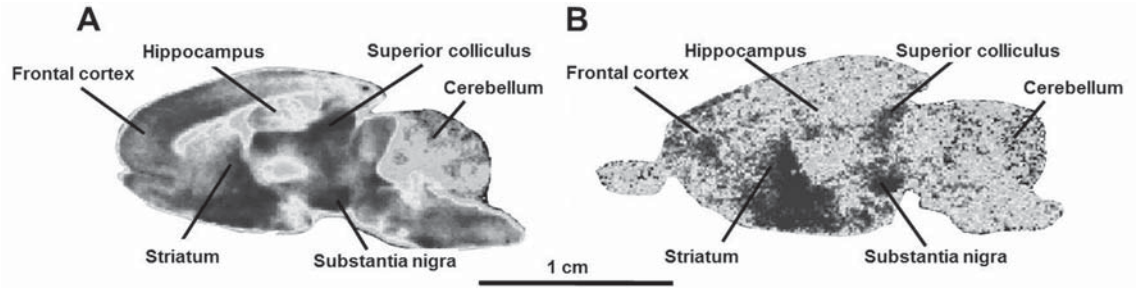

Fig. 14. Comparison of *in vitro* (A) and *ex vivo* (B) autoradiographs of serotonin transporter distribution in rat brain using [^{18}F]FMe-McN5652 as radioligand (adapted from Kretzschmar *et al.* Eur Neuropsychopharmacol 2003[188]).

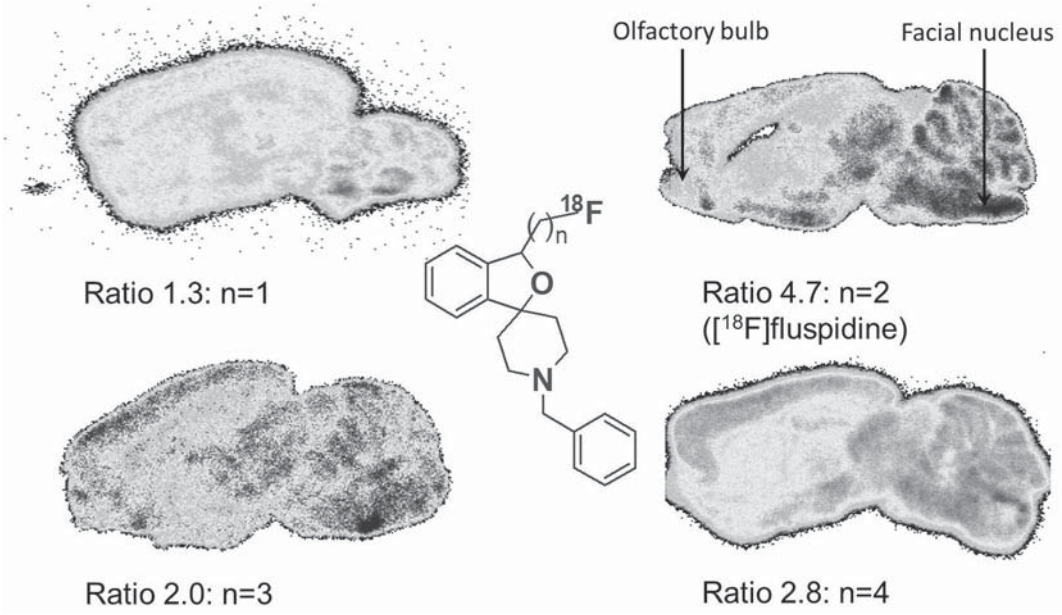

Fig. 15. Comparison of *ex vivo* autoradiographs of σ_1 receptor distribution in rat brain using (±)-[^{18}F]fluspidine and derivatives with various lengths of the alkyl side-chain as radioligands (adapted from Brust *et al.* Curr Med Chem 2014[89]).

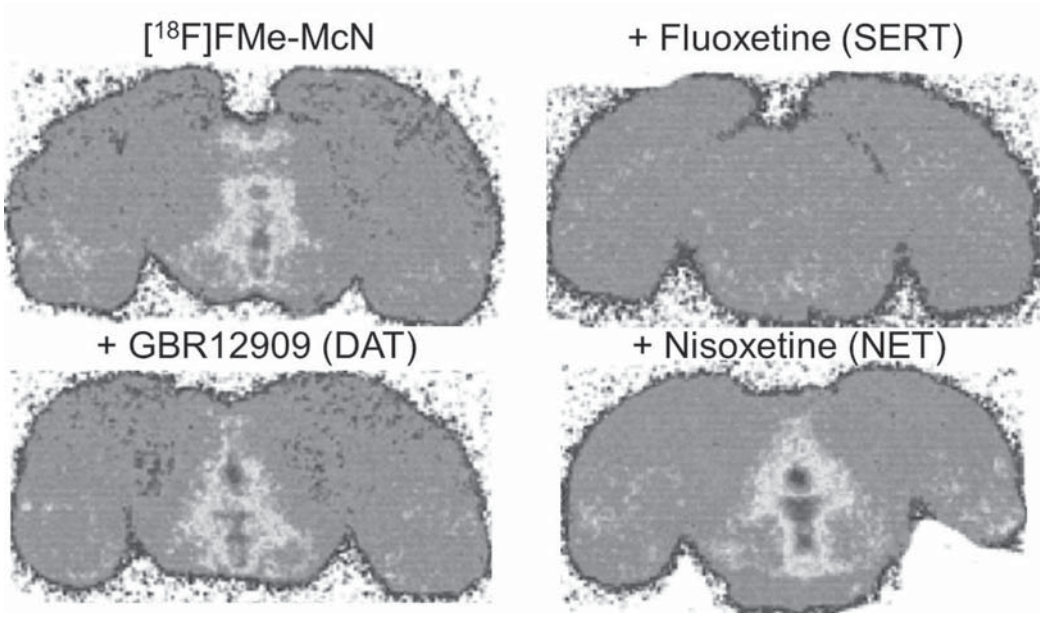

Fig. 16. Comparison of *ex vivo* autoradiographs of serotonin transporter distribution in rat brain using [^{18}F]FMe-McN5652 as radioligand. Specific transporter inhibitors were used to assess the selectivity of transporter binding (adapted from Marjamäki *et al.* Synapse 2003[235]).

in Fig. 16, the selectivity of the new SERT radiotracer [^{18}F]FMe-McN5652 was assessed by *ex vivo* autoradiography performed on rat brain at 120 min after radiotracer injection and 180 min after administration of nisoxetine, a specific norepinephrine uptake inhibitor, or GBR12909, a specific dopamine uptake inhibitor[235]. In contrast to the selective SERT inhibitor fluoxetine, neither drug inhibited binding of [^{18}F]FMe-McN5652 to the rat midbrain, a region with high SERT expression.

In comparison to autoradiography, PET images of

animal brains suffer from low resolution. This can clearly be seen in Fig. 17 where an *ex vivo* autoradiograph of a mouse brain (volume 0.4 mL) is compared to a PET image of a pig brain (volume 110 mL). Despite this limitation, the specificity of radiotracer binding may be determined in animal PET studies. The coronal PET images in Fig. 17 show that administration of the σ_1 receptor ligand SA4503 prevents the specific target binding of (*S*)-[^{18}F]fluspidine in pig brain[236].

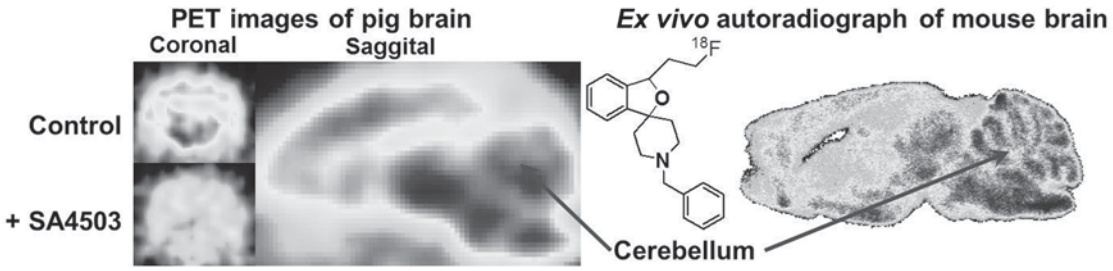

Fig. 17. PET images of a pig brain (left; volume 110 mL) and an *ex vivo* autoradiograph of a mouse brain (right; volume 0.4 mL) are compared to demonstrate the difference in resolution between the two imaging modalities (adapted from Brust *et al.* J Nucl Med 2014[237]).

Estimation of Receptor-binding Parameters in Animals

One of the great advantages of PET is the possibility of precise quantitation of local tracer concentrations in tissue; this ultimately enables the estimation of receptor binding parameters *in vivo*. Preclinical PET studies in animals are suitable for this purpose[7, 8] and hence permit appropriate radiotracer evaluation. Initially, the PET scanner´s resolution was rather low (~10 mm)[238] allowing successful quantitation only in the brains of larger animals such as primates[239, 240], dogs[241-243], cats[244, 245], and pigs[246-248]. During the last decade, various dedicated PET cameras for imaging in small animals have been developed, providing a resolution of 1–2 mm[6, 249].

Moreover, the first PET/MRI systems have become available for both human and small-animal imaging, allowing more accurate identification of brain regions[250]. Thus, accurate quantitation is possible and similar to that achievable with autoradiography[7]. In addition, pharmacokinetic, multiple-tracer, and longitudinal studies can be performed in single subjects constituting a great potential for basic neuroscience research[251], neuropharmacology[8, 252], and the investigation of animal models of neurological and neuropsychiatric disorders[7].

While *in vitro* autoradiography was the method of choice for receptor mapping for more than three decades, the suitability of animal PET/MRI for that purpose has recently been proven. For example, Syvänen[253] determined the $GABA_A$ receptor density, B_{max}, in rat brain using four doses (between 4 μg and 400 μg) of [^{11}C]flumazenil. Five regions with high $GABA_A$ receptor expression were investigated and the highest B_{max} was found in the hippocampus (44 ng/mL) and the lowest in the cerebellum (33 ng/mL). No significant regional differences in the receptor affinity, K_D (5.9 ng/mL), were detected. Using the same setup, an experimental model of epilepsy was investigated and a significant decrease of B_{max} by 12% was reported, while K_D remained unchanged[253].

Although convincing in animals, a similar protocol applied to humans has major drawbacks. Multiple radiotracer injections significantly increase the radiation burden. Furthermore, use of pharmacological doses requires much stronger safety regulations. Therefore, a common and generally-accepted approach to quantify radiotracer receptor binding in humans is estimation of the binding potential, BP = B_{max}/K_D[107]. Assuming that K_D remains unchanged, changes of BP are directly proportional to changes in B_{max}, a postulate which holds in the majority of such studies.

The BP can be estimated by compartmental modeling[254-259]. A compartment model is a linear mathematical model that describes the transfer of a radiotracer among various compartments which are regarded to be

homogenous at all times with respect to the radiotracer concentration. Compartmental models describe the tracer kinetics as a first-order process which is in general, but not always, justified in view of the very low concentrations in which the tracer is present in the investigated organism.

Also, one should keep in mind that the different compartments do not necessarily correspond to unique spaces (e.g. extracellular *versus* intracellular) but usually rather represent different chemical modifications in which the radioactive label resides (see above, the radiotracer and its metabolites). For this reason, all compartmental concentrations in PET are usually referred to the same common volume (total tissue space). This has to be considered when interpreting the numerical results in order to avoid misconceptions. In other words, compartmental models superficially relate tracer concentrations in the different compartments, but in fact represent (local) mass-balance equations. Radiotracer exchange between the different compartments is described by rate constants (usual unit: 1/min) specifying the fractional change of concentration per unit time in the respective compartment due to the process modeled by that specific rate constant.

As long as the tracer kinetics can be considered linear (which is usually a valid assumption) a sufficiently comprehensive compartmental model (with a sufficient number of compartments) will be able to describe any given system. Increasing the number of compartments sufficiently, one can even model diffusive processes (which inherently imply the presence of concentration gradients). For the evaluation of PET data, however, this is not a feasible strategy. It rather turns out that very simple one- or two-tissue compartmental models suffice to adequately describe the data at the given limits of spatial and temporal resolution. For a more in-depth description of the basics of compartmental modeling we refer the reader to the literature[258, 259].

Typical examples of compartmental models are shown in Fig. 18, where C_a refers to the arterial plasma concentration of the unmetabolized radiotracer, M_t to the total amount of radiotracer, M_f to the free fraction, and M_b to the bound fraction. Linear systems of ordinary differential equations describe the changes of radiotracer contents in these models. Based on these equations, the rate constants for the blood-brain and brain-blood transfer (K_1 and k_2' or k_2"), and the rate constants for the specific binding/release (k_3' and k_4), can be estimated by nonlinear least-squares fits. Distribution volumes calculated from the rate constants provide parameters related to receptor density. For the one-tissue compartmental model, the respective parameter is the total distribution volume V_T (equal to K_1/k"$_2$). For the two-tissue compartmental model the total distribution volume $V_T = V_{ND} + V_S = (K_1/k_2')(1 + k_3'/k_4)$, the specific distribution volume $V_S = (K_1/k_2')(k_3'/k_4)$, and the binding potential BP = k_3'/k_4 provide measures of the specific binding.

Fig. 19 shows an example, where a two-tissue compartment model was used to estimate BP of the SERT

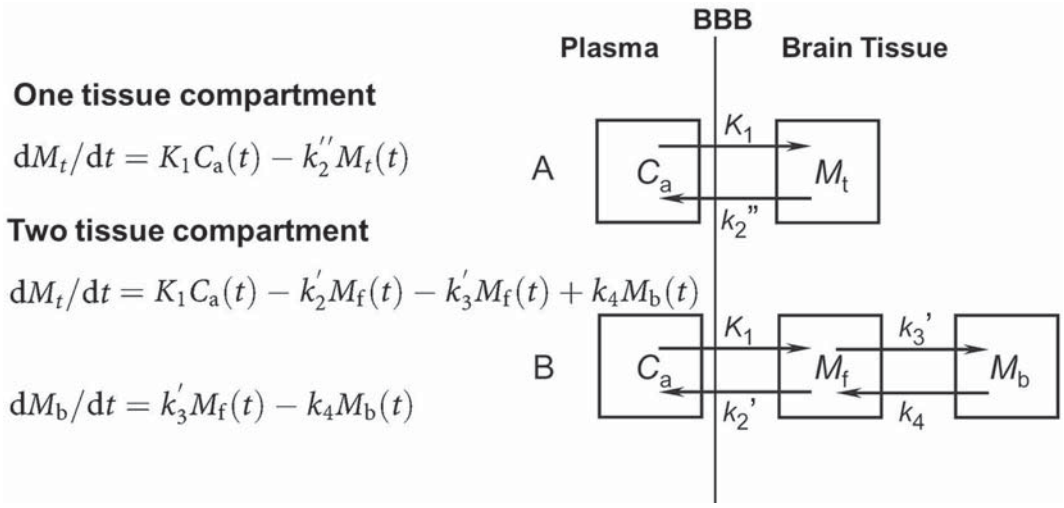

Fig. 18. Compartmental models used to describe receptor binding of radiotracers in brain.

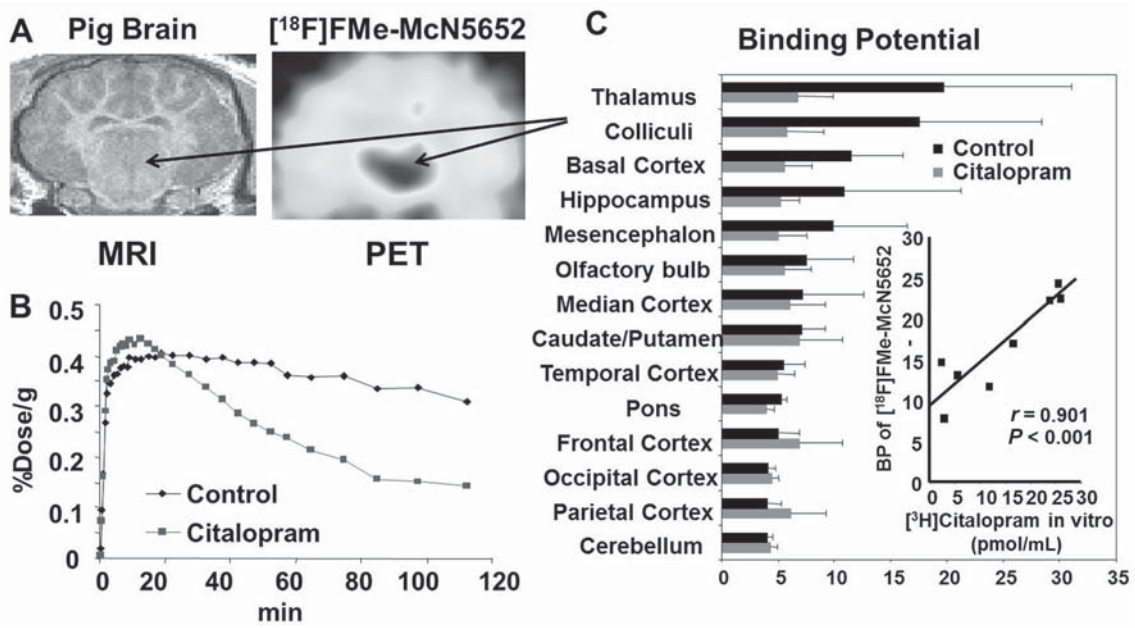

Fig. 19. Comparative PET and autoradiographic study of serotonin distribution in pig brain using [^{18}F]FMe-McN5652 and [^{3}H]citalopram as radioligands. Binding potential values estimated from time-activity curves (B) of a PET study in various brain regions (A) are compared to results from an *in vitro* autoradiographic study using [^{3}H]citalopram (C) (adapted from Brust *et al.* Neuropsychopharmacology 2003[209] and Brust *et al.* Synapse 2003[212]).

radiotracer [^{18}F]FMe-McN5652 in anesthetized pigs under control conditions and after i.v. injection of the highly-selective SERT inhibitor citalopram (5 mg/kg). Under control conditions, BP values clearly reflected the SERT distribution as demonstrated by correlation analysis with [^{3}H]citalopram autoradiography with the highest values in the thalamus and the lowest in the cerebellum. Pre-injection of citalopram significantly inhibited [^{18}F]FMe-McN5652 accumulation, as demonstrated by the time-activity curves, and BP estimated from these curves[209, 260]. This clearly demonstrated the specificity of the radiotracer uptake. The selectivity for the norepinephrine transporter (NET) was demonstrated by pre-injection of maprotilin, a selective NET inhibitor[209].

Accurate measurement of the arterial plasma time-activity curve as well as consideration and correct determination of metabolites in plasma is important for receptor quantitation based on compartmental models using an arterial input function. This poses substantial problems in imaging of small animals and humans. Therefore, alternative quantification strategies, called "references tissue models'' have been developed[261, 262]. These models rest on the observation that (apart from minor effects of different arrival times) the arterial input function is identical in different brain regions. Then, it is possible to use the tissue response to this input function in one region as an indirect measure of the input function if that region is devoid of the targeted receptor. This obviates the need for actual measurement of the arterial plasma time-activity curve and also makes metabolite analysis unnecessary. Furthermore, this strategy can be used even in the presence of brain metabolites. Although these techniques have several advantages compared to arterial blood sampling (especially non-invasiveness), they quite sensitively rely on several assumptions and should be used with great care. For example, the existence of any specific binding in the reference region results in an underestimation of specific binding in the target region[257].

PET also allows the visualization of specific receptor binding by estimation of the binding parameters in each voxel, i.e. each image point in the three-dimensional rectangular grid[263]. The higher the number of voxels, the higher the number of calculations to be executed. To be able to perform about a million estimations in a

reasonable time, graphical methods are available allowing linear rather than non-linear regression. For radiotracers with irreversible binding the Gjedde-Patlak graphical analysis[264-266] and for those with reversible binding the Logan graphical analysis[267] have become the methods of choice. For the two-tissue compartmental model, the slope of the regression line in the Logan plot represents the total distribution volume V_T, defined by $K_1/k_2(1+k_3/k_4)$ + fbv (fbv = fractional blood volume in the target region, k_3/k_4 = BP[267]).

Fig. 20A shows a parametric map of V_T of the α7 nAChR radiotracer [^{18}F]NS10743 resampled into the MR-based common stereotactic space for the brain of a juvenile pig[230]. Fig. 20B shows V_T of [^{18}F]NS10743 after administration of the selective α7 nAChR antagonist NS6740. This clearly demonstrates specific radiotracer binding in pig brain.

Newer developments include proposals to obtain parametric images even in cases without either an arterial input function or a reference region[268], direct reconstruction algorithms of linear and nonlinear parametric images, and joint estimation of parametric images and input function[263]. Further validation of these concepts is still needed.

Proof-of-Concept in Humans

The final step in PET radiotracer development is proof-of-concept in humans. A prerequisite to get permission for such studies is the transition of the biomarker from research-grade radiochemical to a radiopharmaceutical, for which higher standards of product quality must be met[269]. Many aspects of radiation safety, toxicology issues, quality control, licensing, and regulatory control need to be considered for the production of radiopharmaceuticals and these have been extensively reviewed elsewhere[5, 100, 270, 271]. The regulatory framework has become increasingly restrictive during the last two decades. Therefore, the time between first successful radiosynthesis of a new PET radiotracer and its first human use is at least between 5 and 10 years. For example, in the case of the α4β2 nAChR radiotracer (–)-[^{18}F]flubatine, the time between the first report on radiosynthesis[164] and the first report on human use[16] was 8 years. For [^{18}F]FMe-McN5652 it was 10 years[210, 272], and for [^{18}F]FEOBV[126], a radiotracer for the VAChT, it has been almost 20 years[273]. At the beginning of neuroreceptor imaging with PET this transition time was much shorter, in the range of 1–2 years as exemplified by [^{11}C]raclopride[225, 274], 3-*N*-[^{11}C]methylspiperone[224], and [^{11}C]flumazenil[49, 275].

However, even if a radiotracer is not further developed into a radiopharmaceutical for imaging in human subjects it may find widespread use in preclinical studies with special animal PET devices[276] to investigate animal models of diseases[7] or new drugs[8, 252].

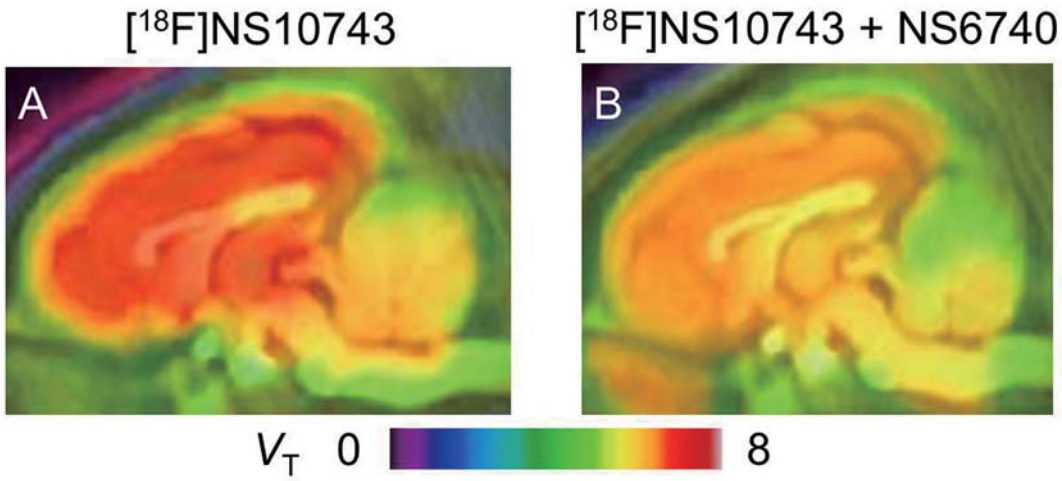

Fig. 20. Parametric maps of the distribution volumes (V_T, mL/g) of [^{18}F]NS10743 under baseline (A) and blocking (B) conditions in sagittal plane of pig brain. The V_T values were calculated by the classic Logan method using the arterial input function for [^{18}F]NS10743 (adapted from Deuther-Conrad *et al.* Eur J Nucl Med Mol Imaging 2011[230]).

Conclusion

The main focus of this review is the development and evaluation of radiolabeled ligands (radiotracers) in order to investigate brain functions in living organisms. Application of radiotracers provides images of transport, metabolic, and neurotransmission processes on the molecular level. PET is a method used in humans to acquire such information. It is the most sensitive and specific molecular *in vivo* imaging method available at present. Through the integration of chemical/radiochemical, pharmaceutical/radiopharmaceutical, biochemical and radiopharmacological basic research, computational chemistry, and with the aid of nuclear medicine diagnostics, a new approach in neuroscience has been made available. The foremost importance of this approach is the diagnosis and therapeutic monitoring of brain diseases.

ACKNOWLEDGEMENTS

Many valuable contributions of our colleagues at HZDR are gratefully acknowledged.

Received date: 2014-04-19; Accepted date: 2014-06-02

REFERENCES

[1] Mankoff DA. A definition of molecular imaging. J Nucl Med 2007, 48: 18N, 21N.

[2] Pichler BJ, Judenhofer MS, Pfannenberg C. Multimodal imaging approaches: PET/CT and PET/MRI. Handb Exp Pharmacol 2008: 109–132.

[3] Drzezga A, Barthel H, Minoshima S, Sabri O. Potential clinical applications of PET/MR imaging in neurodegenerative diseases. J Nucl Med 2014, 55: 1–9.

[4] Levi H. George von Hevesy memorial lecture. George Hevesy and his concept of radioactive indicators--in retrospect. Eur J Nucl Med 1976, 1: 3–10.

[5] Sampson CD (Ed.). Textbook of Radiopharmacy: Theory and Practice. 3rd. ed. Amsterdam: Gordan and Breach Science Publishers, 1999.

[6] Brust P, Deuther-Conrad W, Donat CK, Barthel H, Riss P, Paterson L, *et al.* Preclinical aspects of nicotinic acetylcholine receptor imaging. In: Dierckx RAJ, Otte A, de Vries EFJ, *et al.* (Eds.). PET and SPECT of Neurobiological Systems. Springer, 2014: 465–512.

[7] Virdee K, Cumming P, Caprioli D, Jupp B, Rominger A, Aigbirhio FI, *et al.* Applications of positron emission tomography in animal models of neurological and neuropsychiatric disorders. Neurosci Biobehav Rev 2012, 36: 1188–1216.

[8] Melhem M. Translation of central nervous system occupancy from animal models: application of pharmacokinetic/pharmacodynamic modeling. J Pharmacol Exp Ther 2013, 347: 2–6.

[9] Frey KA, Koeppe RA, Mulholland GK, Jewett D, Hichwa R, Ehrenkaufer RL, *et al. In vivo* muscarinic cholinergic receptor imaging in human brain with [^{11}C]scopolamine and positron emission tomography. J Cereb Blood Flow Metab 1992, 12: 147–154.

[10] Xie G, Gunn RN, Dagher A, Daloze T, Plourde G, Backman SB, *et al.* PET quantification of muscarinic cholinergic receptors with [N-11C-methyl]-benztropine and application to studies of propofol-induced unconsciousness in healthy human volunteers. Synapse 2004, 51: 91–101.

[11] Yamamoto S, Ouchi Y, Nakatsuka D, Tahara T, Mizuno K, Tajima S, *et al.* Reduction of [^{11}C](+)3-MPB binding in brain of chronic fatigue syndrome with serum autoantibody against muscarinic cholinergic receptor. PLoS One 2012, 7: e51515.

[12] Ichise M, Cohen RM, Carson RE. Noninvasive estimation of normalized distribution volume: application to the muscarinic-2 ligand [^{18}F]FP-TZTP. J Cereb Blood Flow Metab 2008, 28: 420–430.

[13] Sabri O, Kendziorra K, Wolf H, Gertz HJ, Brust P. Acetylcholine receptors in dementia and mild cognitive impairment. Eur J Nucl Med Mol Imaging 2008, 35 Suppl 1: S30–45.

[14] Ding YS, Fowler JS, Logan J, Wang GJ, Telang F, Garza V, *et al.* 6-[^{18}F]Fluoro-A-85380, a new PET tracer for the nicotinic acetylcholine receptor: studies in the human brain and *in vivo* demonstration of specific binding in white matter. Synapse 2004, 53: 184–189.

[15] Wong DF, Kuwabara H, Kim J, Brasic JR, Chamroonrat W, Gao Y, *et al.* PET imaging of high-affinity $\alpha_4\beta_2$ nicotinic acetylcholine receptors in humans with ^{18}F-AZAN, a radioligand with optimal brain kinetics. J Nucl Med 2013, 54: 1308–1314.

[16] Sabri O, Wilke S, Gräf S, Schönknecht P, Becker G, Patt M, *et al.* Cerebral $\alpha_4\beta_2$ nicotinic acetylcholine receptors (nAChRs) in early Alzheimer disease (AD) assessed with the new PET tracer (-)-[^{18}F]-norchloro-fluoro-homoepibatidine (NCFHEB). J Nucl Med 2011, 52 (Suppl. 1): 1267.

[17] Toyohara J, Sakata M, Wu J, Ishikawa M, Oda K, Ishii K, *et al.* Preclinical and the first clinical studies on [^{11}C] CHIBA-1001 for mapping α7 nicotinic receptors by positron emission tomography. Ann Nucl Med 2009, 23: 301–309.

[18] Bauer A, Holschbach MH, Meyer PT, Boy C, Herzog H, Olsson RA, *et al. In vivo* imaging of adenosine A_1 receptors in the human brain with [^{18}F]CPFPX and positron emission

tomography. Neuroimage 2003, 19: 1760–1769.

[19] Fukumitsu N, Ishii K, Kimura Y, Oda K, Hashimoto M, Suzuki M, *et al.* Adenosine A_1 receptors using 8-dicyclopropylmethyl-1-[^{11}C]methyl-3-propylxanthine PET in Alzheimer's disease. Ann Nucl Med 2008, 22: 841–847.

[20] Mishina M, Ishiwata K, Naganawa M, Kimura Y, Kitamura S, Suzuki M, *et al.* Adenosine A_{2A} receptors measured with [^{11}C] TMSX PET in the striata of Parkinson's disease patients. PLoS One 2011, 6: e17338.

[21] Ramlackhansingh AF, Bose SK, Ahmed I, Turkheimer FE, Pavese N, Brooks DJ. Adenosine 2_A receptor availability in dyskinetic and nondyskinetic patients with Parkinson disease. Neurology 2011, 76: 1811–1816.

[22] Burns HD, Van Laere K, Sanabria-Bohorquez S, Hamill TG, Bormans G, Eng WS, *et al.* [^{18}F]MK-9470, a positron emission tomography (PET) tracer for *in vivo* human PET brain imaging of the cannabinoid-1 receptor. Proc Natl Acad Sci U S A 2007, 104: 9800–9805.

[23] Terry GE, Hirvonen J, Liow JS, Seneca N, Tauscher JT, Schaus JM, *et al.* Biodistribution and dosimetry in humans of two inverse agonists to image cannabinoid CB1 receptors using positron emission tomography. Eur J Nucl Med Mol Imaging 2010, 37: 1499–1506.

[24] Wong DF, Kuwabara H, Horti AG, Raymont V, Brasic J, Guevara M, *et al.* Quantification of cerebral cannabinoid receptors subtype 1 (CB1) in healthy subjects and schizophrenia by the novel PET radioligand [^{11}C]OMAR. Neuroimage 2010, 52: 1505–1513.

[25] Ahmad R, Koole M, Evens N, Serdons K, Verbruggen A, Bormans G, *et al.* Whole-body biodistribution and radiation dosimetry of the cannabinoid type 2 receptor ligand [^{11}C]-NE40 in healthy subjects. Mol Imaging Biol 2013.

[26] Farde L, Halldin C, Stone-Elander S, Sedvall G. PET analysis of human dopamine receptor subtypes using ^{11}C-SCH 23390 and ^{11}C-raclopride. Psychopharmacology 1987, 92: 278–284.

[27] Karlsson P, Farde L, Halldin C, Swahn CG, Sedvall G, Foged C, *et al.* PET examination of [^{11}C]NNC 687 and [^{11}C] NNC 756 as new radioligands for the D_1-dopamine receptor. Psychopharmacology 1993, 113: 149–156.

[28] Slifstein M, Kolachana B, Simpson EH, Tabares P, Cheng B, Duvall M, *et al.* COMT genotype predicts cortical-limbic D_1 receptor availability measured with [^{11}C]NNC112 and PET. Mol Psychiatry 2008, 13: 821–827.

[29] Farde L, Hall H, Ehrin E, Sedvall G. Quantitative analysis of D_2 dopamine receptor binding in the living human brain by PET. Science 1986, 231: 258–261.

[30] Wong DF, Wagner HN, Jr., Tune LE, Dannals RF, Pearlson GD, Links JM, *et al.* Positron emission tomography reveals elevated D_2 dopamine receptors in drug-naive schizophrenics. Science 1986, 234: 1558–1563.

[31] Narendran R, Frankle WG, Mason NS, Laymon CM, Lopresti BJ, Price JC, *et al.* Positron emission tomography imaging of $D_{2/3}$ agonist binding in healthy human subjects with the radiotracer [^{11}C]-N-propyl-norapomorphine: preliminary evaluation and reproducibility studies. Synapse 2009, 63: 574–584.

[32] Otsuka T, Ito H, Halldin C, Takahashi H, Takano H, Arakawa R, *et al.* Quantitative PET analysis of the dopamine D_2 receptor agonist radioligand ^{11}C-(R)-2-CH3O-N-n-propylnorapomorphine in the human brain. J Nucl Med 2009, 50: 703–710.

[33] Farde L, Suhara T, Nyberg S, Karlsson P, Nakashima Y, Hietala J, *et al.* A PET-study of [^{11}C]FLB 457 binding to extrastriatal D_2-dopamine receptors in healthy subjects and antipsychotic drug-treated patients. Psychopharmacology 1997, 133: 396–404.

[34] Mukherjee J, Christian BT, Dunigan KA, Shi B, Narayanan TK, Satter M, *et al.* Brain imaging of ^{18}F-fallypride in normal volunteers: blood analysis, distribution, test-retest studies, and preliminary assessment of sensitivity to aging effects on dopamine D-2/D-3 receptors. Synapse 2002, 46: 170–188.

[35] Ginovart N, Willeit M, Rusjan P, Graff A, Bloomfield PM, Houle S, *et al.* Positron emission tomography quantification of [^{11}C]-(+)-PHNO binding in the human brain. J Cereb Blood Flow Metab 2007, 27: 857–871.

[36] Moresco RM, Scheithauer BW, Lucignani G, Lombardi D, Rocca A, Losa M, *et al.* Oestrogen receptors in meningiomas: a correlative PET and immunohistochemical study. Nucl Med Comm 1997, 18: 606–615.

[37] Toyohara J, Sakata M, Fujinaga M, Yamasaki T, Oda K, Ishii K, *et al.* Preclinical and the first clinical studies on [^{11}C] ITMM for mapping metabotropic glutamate receptor subtype 1 by positron emission tomography. Nucl Med Biol 2013, 40: 214–220.

[38] Ametamey SM, Treyer V, Streffer J, Wyss MT, Schmidt M, Blagoev M, *et al.* Human PET studies of metabotropic glutamate receptor subtype 5 with ^{11}C-ABP688. J Nucl Med 2007, 48: 247–252.

[39] Brown AK, Kimura Y, Zoghbi SS, Simeon FG, Liow JS, Kreisl WC, *et al.* Metabotropic glutamate subtype 5 receptors are quantified in the human brain with a novel radioligand for PET. J Nucl Med 2008, 49: 2042–2048.

[40] Kagedal M, Cselenyi Z, Nyberg S, Jonsson S, Raboisson P, Stenkrona P, *et al.* Non-linear mixed effects modelling of positron emission tomography data for simultaneous estimation of radioligand kinetics and occupancy in healthy volunteers. Neuroimage 2012, 61: 849–856.

[41] Wong DF, Waterhouse R, Kuwabara H, Kim J, Brasic JR, Chamroonrat W, *et al.* ^{18}F-FPEB, a PET radiopharmaceutical for quantifying metabotropic glutamate 5 receptors: a first-

in-human study of radiochemical safety, biokinetics, and radiation dosimetry. J Nucl Med 2013, 54: 388–396.

[42] Kumlien E, Hartvig P, Valind S, Oye I, Tedroff J, Langström B. NMDA-receptor activity visualized with (*S*)-[N-methyl-^{11}C] ketamine and positron emission tomography in patients with medial temporal lobe epilepsy. Epilepsia 1999, 40: 30–37.

[43] Hammers A, Asselin M, Brooks DJ, Luthra SK, Hume SP, Thompson PJ*, et al.* Correlation of memory function with binding of [C-11]CNS 5161, a novel putative NMDA ion channel PET ligand. Neuroimage 2004, 22(Suppl 2): T54–55.

[44] Ametamey SM, Bruehlmeier M, Kneifel S, Kokic M, Honer M, Arigoni M*, et al.* PET studies of ^{18}F-memantine in healthy volunteers. Nucl Med Biol 2002, 29: 227–231.

[45] McGinnity CJ, Hammers A, Riano Barros DA, Luthra SK, Jones PA, Trigg W*, et al.* Initial evaluation of ^{18}F-GE-179, a putative PET Tracer for activated N-methyl D-aspartate receptors. J Nucl Med 2014, 55: 423–430.

[46] Matsumoto R, Haradahira T, Ito H, Fujimura Y, Seki C, Ikoma Y*, et al.* Measurement of glycine binding site of N-methyl-D-asparate receptors in living human brain using 4-acetoxy derivative of L-703,717, 4-acetoxy-7-chloro-3-[3-(4-[^{11}C] methoxybenzyl) phenyl]-2(1H)-quinolone (AcL703) with positron emission tomography. Synapse 2007, 61: 795–800.

[47] Yanai K, Watanabe T, Itoh M, Hatazawa J, Iwata R, Ido T. Labeling of histamine H1-receptors *in vivo*: a compartment model analysis and positron emission tomographic imaging. Agents Actions Suppl 1991, 33: 381–386.

[48] Ashworth S, Rabiner EA, Gunn RN, Plisson C, Wilson AA, Comley RA*, et al.* Evaluation of ^{11}C-GSK189254 as a novel radioligand for the H3 receptor in humans using PET. J Nucl Med 2010, 51: 1021–1029.

[49] Persson A, Ehrin E, Eriksson L, Farde L, Hedström CG, Litton JE*, et al.* Imaging of [^{11}C]-labelled Ro 15-1788 binding to benzodiazepine receptors in the human brain by positron emission tomography. J Psychiatric Res 1985, 19: 609–622.

[50] Leveque P, Sanabria-Bohorquez S, Bol A, De Volder A, Labar D, Van Rijckevorsel K*, et al.* Quantification of human brain benzodiazepine receptors using [^{18}F]fluoroethylflumazenil: a first report in volunteers and epileptic patients. Eur J Nucl Med Mol Imaging 2003, 30: 1630–1636.

[51] Lee JD, Park HJ, Park ES, Kim DG, Rha DW, Kim EY*, et al.* Assessment of regional $GABA_A$ receptor binding using ^{18}F-fluoroflumazenil positron emission tomography in spastic type cerebral palsy. Neuroimage 2007, 34: 19–25.

[52] Massaweh G, Schirrmacher E, la Fougere C, Kovacevic M, Wängler C, Jolly D*, et al.* Improved work-up procedure for the production of [^{18}F]flumazenil and first results of its use with a high-resolution research tomograph in human stroke. Nucl Med Biol 2009, 36: 721–727.

[53] Lingford-Hughes A, Hume SP, Feeney A, Hirani E, Osman S, Cunningham VJ*, et al.* Imaging the GABA-benzodiazepine receptor subtype containing the alpha5-subunit *in vivo* with [^{11}C]Ro15 4513 positron emission tomography. J Cereb Blood Flow Metab 2002, 22: 878–889.

[54] Frost JJ, Mayberg HS, Sadzot B, Dannals RF, Lever JR, Ravert HT*, et al.* Comparison of [^{11}C]diprenorphine and [^{11}C] carfentanil binding to opiate receptors in humans by positron emission tomography. J Cereb Blood Flow Metab 1990, 10: 484–492.

[55] Madar I, Lesser RP, Krauss G, Zubieta JK, Lever JR, Kinter CM*, et al.* Imaging of σ- and μ-opioid receptors in temporal lobe epilepsy by positron emission tomography. Ann Neurol 1997, 41: 358–367.

[56] Tomasi G, Zheng M-Q, Weinzimmer D, Lin S-F, Nabulsi N, Williams W*, et al.* Kinetic modeling of the kappa agonist tracer [^{11}C]GR103545 in humans. J Nucl Med 2010, 51 (Supplement 2): 1293.

[57] Cohen RM, Carson RE, Sunderland T. Opiate receptor avidity in the thalamus is sexually dimorphic in the elderly. Synapse 2000, 38: 226–229.

[58] Baumgärtner U, Buchholz HG, Bellosevich A, Magerl W, Siessmeier T, Rolke R*, et al.* High opiate receptor binding potential in the human lateral pain system. Neuroimage 2006, 30: 692–699.

[59] Hostetler ED, Sanabria-Bohorquez S, Fan H, Zeng Z, Gantert L, Williams M*, et al.* Synthesis, characterization, and monkey positron emission tomography (PET) studies of [^{18}F]Y1-973, a PET tracer for the neuropeptide Y Y_1 receptor. Neuroimage 2011, 54: 2635–2642.

[60] Pike VW, McCarron JA, Lammerstma AA, Hume SP, Poole K, Grasby PM*, et al.* First delineation of 5-HT_{1A} receptors in human brain with PET and ^{11}C WAY-100635. Eur J Pharmacol 1995, 283: R1–3.

[61] Parsey RV, Slifstein M, Hwang DR, Abi-Dargham A, Simpson N, Mawlawi O*, et al.* Validation and reproducibility of measurement of 5-HT_{1A} receptor parameters with [carbonyl-^{11}C]WAY-100635 in humans: comparison of arterial and reference tisssue input functions. J Cereb Blood Flow Metab 2000, 20: 1111–1133.

[62] Andree B, Halldin C, Pike VW, Gunn RN, Olsson H, Farde L. The PET radioligand [carbonyl-^{11}C]desmethyl-WAY-100635 binds to 5-HT_{1A} receptors and provides a higher radioactive signal than [carbonyl-^{11}C]WAY-100635 in the human brain. J Nucl Med 2002, 43: 292–303.

[63] Houle S, Wilson AA, Inaba T, Fisher N, DaSilva JN. Imaging 5-HT_{1A} receptors with positron emission tomography: initial human studies with [^{11}C]CPC-222. Nucl Med Comm 1997, 18: 1130–1134.

[64] Milak MS, DeLorenzo C, Zanderigo F, Prabhakaran J, Kumar JS, Majo VJ*, et al. In vivo* quantification of human serotonin

1A receptor using ^{11}C-CUMI-101, an agonist PET radiotracer. J Nucl Med 2010, 51: 1892–1900.

[65] Costes N, Merlet I, Zimmer L, Lavenne F, Cinotti L, Delforge J*, et al.* Modeling [^{18} F]MPPF positron emission tomography kinetics for the determination of 5-hydroxytryptamine$_{1A}$ receptor concentration with multiinjection. J Cereb Blood Flow Metab 2002, 22: 753–765.

[66] Theodore WH, Giovacchini G, Bonwetsch R, Bagic A, Reeves-Tyer P, Herscovitch P*, et al.* The effect of antiepileptic drugs on 5-HT-receptor binding measured by positron emission tomography. Epilepsia 2006, 47: 499–503.

[67] Gallezot JD, Nabulsi N, Neumeister A, Planeta-Wilson B, Williams WA, Singhal T*, et al.* Kinetic modeling of the serotonin 5-HT$_{1B}$ receptor radioligand [^{11}C]P943 in humans. J Cereb Blood Flow Metab 2010, 30: 196–210.

[68] Varnäs K, Nyberg S, Halldin C, Varrone A, Takano A, Karlsson P*, et al.* Quantitative analysis of [^{11}C]AZ10419369 binding to 5-HT$_{1B}$ receptors in human brain. J Cereb Blood Flow Metab 2011, 31: 113–123.

[69] Murrough JW, Henry S, Hu J, Gallezot JD, Planeta-Wilson B, Neumaier JF*, et al.* Reduced ventral striatal/ventral pallidal serotonin1B receptor binding potential in major depressive disorder. Psychopharmacology 2011, 213: 547–553.

[70] Hinz R, Bhagwagar Z, Cowen PJ, Cunningham VJ, Grasby PM. Validation of a tracer kinetic model for the quantification of 5-HT$_{2A}$ receptors in human brain with [^{11}C]MDL 100,907. J Cereb Blood Flow Metab 2007, 27: 161–172.

[71] Rosier A, Dupont P, Peuskens J, Bormans G, Vandenberghe R, Maes M*, et al.* Visualisation of loss of 5-HT$_{2A}$ receptors with age in healthy volunteers using [^{18}F]altanserin and positron emission tomographic imaging. Psychiatry Res 1996, 68: 11–22.

[72] van Dyck CH, Soares JC, Tan PZ, Staley JK, Baldwin RM, Amici LA*, et al.* Equilibrium modeling of 5-HT$_{2A}$ receptors with [^{18}F]deuteroaltanserin and PET: feasibility of a constant infusion paradigm. Nucl Med Biol 2000, 27: 715–722.

[73] Trichard C, Paillere-Martinot ML, Attar-Levy D, Recassens C, Monnet F, Martinot JL. Binding of antipsychotic drugs to cortical 5-HT$_{2A}$ receptors: a PET study of chlorpromazine, clozapine, and amisulpride in schizophrenic patients. Am J Psychiatry 1998, 155: 505–508.

[74] Ettrup A, da Cunha-Bang S, McMahon B, Lehel S, Dyssegaard A, Skibsted AW*, et al.* Serotonin 2$_A$ receptor agonist binding in the human brain with [^{11}C]Cimbi-36. J Cereb Blood Flow Metab 2014.

[75] Marner L, Gillings N, Comley RA, Baare WF, Rabiner EA, Wilson AA*, et al.* Kinetic modeling of ^{11}C-SB207145 binding to 5-HT$_4$ receptors in the human brain *in vivo*. J Nucl Med 2009, 50: 900–908.

[76] Parker CA, Gunn RN, Rabiner EA, Slifstein M, Comley R, Salinas C*, et al.* Radiosynthesis and characterization of ^{11}C-GSK215083 as a PET radioligand for the 5-HT$_6$ receptor. J Nucl Med 2012, 53: 295–303.

[77] Mishina M, Ishiwata K, Ishii K, Kitamura S, Kimura Y, Kawamura K, *et al*. Function of sigma1 receptors in Parkinson's disease. Acta Neurol Scand 2005 112: 103–107.

[78] Waterhouse RN, Nobler MS, Zhou Y, Chang RC, Morales O, Kuwabara H*, et al.* First evaluation of the sigma1 receptor radioligand [^{18}F]1-3-fluoropropyl-4-((4-cyanophenoxy)-methyl) piperidine ([^{18}F]FPS) in healthy humans. Neuroimage 2004, 22: T29.

[79] Junck L, Olson JM, Ciliax BJ, Koeppe RA, Watkins GL, Jewett DM*, et al.* PET imaging of human gliomas with ligands for the peripheral benzodiazepine binding site. Ann Neurol 1989, 26: 752–758.

[80] Banati RB, Goerres GW, Myers R, Gunn RN, Turkheimer FE, Kreutzberg GW*, et al*. [^{11}C](R)-PK11195 positron emission tomography imaging of activated microglia *in vivo* in Rasmussen's encephalitis. Neurology 1999, 53: 2199–2203.

[81] Brown AK, Fujita M, Fujimura Y, Liow JS, Stabin M, Ryu YH*, et al.* Radiation dosimetry and biodistribution in monkey and man of ^{11}C-PBR28: a PET radioligand to image inflammation. J Nucl Med 2007, 48: 2072–2079.

[82] Endres CJ, Pomper MG, James M, Uzuner O, Hammoud DA, Watkins CC*, et al.* Initial evaluation of ^{11}C-DPA-713, a novel TSPO PET ligand, in humans. J Nucl Med 2009, 50: 1276–1282.

[83] Yasuno F, Kosaka J, Ota M, Higuchi M, Ito H, Fujimura Y*, et al.* Increased binding of peripheral benzodiazepine receptor in mild cognitive impairment-dementia converters measured by positron emission tomography with [^{11}C]DAA1106. Psychiatry Res 2012, 203: 67–74.

[84] Gulyas B, Toth M, Schain M, Airaksinen A, Vas A, Kostulas K*, et al.* Evolution of microglial activation in ischaemic core and peri-infarct regions after stroke: a PET study with the TSPO molecular imaging biomarker [^{11}C]vinpocetine. J Neurol Sci 2012, 320: 110–117.

[85] Fujimura Y, Zoghbi SS, Simeon FG, Taku A, Pike VW, Innis RB, *et al.* Quantification of translocator protein (18 kDa) in the human brain with PET and a novel radioligand, F-18-PBR06. J Nucl Med 2009, 50: 1047–1053.

[86] Arlicot N, Vercouillie J, Ribeiro MJ, Tauber C, Venel Y, Baulieu JL*, et al.* Initial evaluation in healthy humans of [^{18}F] DPA-714, a potential PET biomarker for neuroinflammation. Nucl Med Biol 2012, 39: 570–578.

[87] Mizrahi R, Rusjan PM, Kennedy J, Pollock B, Mulsant B, Suridjan I*, et al.* Translocator protein (18 kDa) polymorphism (rs6971) explains in-vivo brain binding affinity of the PET radioligand [^{18}F]FEPPA. J Cereb Blood Flow Metab 2012, 32: 968–972.

[88] Guo Q, Colasanti A, Owen DR, Onega M, Kamalakaran A, Bennacef I*, et al*. Quantification of the specific translocator protein signal of ^{18}F-PBR111 in healthy humans: a genetic polymorphism effect on *in vivo* binding. J Nucl Med 2013, 54: 1915–1923.

[89] Brust P, Deuther-Conrad W, Lehmkuhl K, Jia H, Wünsch B. Molecular imaging of σ_1 receptors *in vivo*: current status and perspectives. Curr Med Chem 2014, 21: 35-69.

[90] Jansen KL, Faull RL, Storey P, Leslie RA. Loss of sigma binding sites in the CA1 area of the anterior hippocampus in Alzheimer's disease correlates with CA1 pyramidal cell loss. Brain Res 1993, 623: 299-302.

[91] Weissman AD, Casanova MF, Kleinman JE, London ED, De Souza EB. Selective loss of cerebral cortical sigma, but not PCP binding sites in schizophrenia. Biol Psychiatry 1991, 29: 41–54.

[92] van Waarde A, Rybczynska AA, Ramakrishnan N, Ishiwata K, Elsinga PH, Dierckx RA. Sigma receptors in oncology: therapeutic and diagnostic applications of sigma ligands. Curr Pharm Des 2010, 16: 3519–3537.

[93] Banister SD, Kassiou M. The therapeutic potential of sigma (σ) receptors for the treatment of central nervous system diseases: evaluation of the evidence. Curr Pharm Des 2012, 18: 884–901.

[94] Megalizzi V, Le Mercier M, Decaestecker C. Sigma receptors and their ligands in cancer biology: overview and new perspectives for cancer therapy. Med Res Rev 2012, 32: 410–427.

[95] Schliebs R, Arendt T. The cholinergic system in aging and neuronal degeneration. Behav Brain Res 2011, 221: 555–563.

[96] Brust P, Deuther-Conrad W. Molecular imaging of α7 nicotinic acetylcholine receptors *in vivo*: current status and perspectives. In: Bright P (Ed). Neuroimaging - Clinical Applications. InTech, 2012: 533–558.

[97] Brust P, Peters D, Deuther-Conrad W. Development of radioligands for the imaging of α7 nicotinic acetylcholine receptors with positron emission tomography. Curr Drug Targets 2012, 13: 594–601.

[98] Kadir A, Almkvist O, Wall A, Langström B, Nordberg A. PET imaging of cortical ^{11}C-nicotine binding correlates with the cognitive function of attention in Alzheimer's disease. Psychopharmacology 2006, 188: 509–520.

[99] Papke RL. Merging old and new perspectives on nicotinic acetylcholine receptors. Biochem Pharmacol 2014. doi: 10.1016/j.bcp.2014.1001.1029.

[100] Moerlein SM. Molecular imaging and the development of new radiopharmaceuticals. In: Kowalsky RJ, Falen SW (Eds.). Radiopharmaceuticals in Nuclear Pharmacy and Nuclear Medicine. American Pharmacists Association (APhA), 2011: 741.

[101] Davenport AP, Russel FD. Radioligand Binding Assays: Theory and Practice. In: Mather SJ (Ed.). Current Directions in Radiopharmaceutical Research and Development. Kluwer Academic Publisher, 1996: 169–179.

[102] Koeppe RA. A panel discussion on the future of pharmacology and experimental tomography. In: Gjedde A, Hansen SB, Knudsen GM, Paulson OB (Eds.). Physiological Imaging of the Brain with PET. Academic Press, 2001: 402.

[103] Hurst R, Rollema H, Bertrand D. Nicotinic acetylcholine receptors: from basic science to therapeutics. Pharmacol Ther 2013, 137: 22–54.

[104] Lendvai B, Kassai F, Szajli A, Nemethy Z. alpha7 Nicotinic acetylcholine receptors and their role in cognition. Brain Res Bull 2013, 93: 86–96.

[105] Sorger D, Scheunemann M, Vercouillie J, Grossmann U, Fischer S, Hiller A*, et al*. Neuroimaging of the vesicular acetylcholine transporter by a novel 4-[^{18}F]fluoro-benzoyl derivative of 7-hydroxy-6-(4-phenyl-piperidin-1-yl)-octahydro-benzo[1,4]oxazines. Nucl Med Biol 2009, 36: 17–27.

[106] Giboureau N, Som IM, Boucher-Arnold A, Guilloteau D, Kassiou M. PET radioligands for the vesicular acetylcholine transporter (VAChT). Curr Top Med Chem 2010, 10: 1569–1583.

[107] Fujita M, Innis RB. *In vivo* molecular imaging: ligand development and research applications. In: Borroni E and Kupfer DJ (Eds.). Neuropsychopharmacology: The Fifth Generation of Progress. New York: Raven Press Ltd, 2002, Section 3: 411–425.

[108] Blower PJ. Microautoradiography. In: Mather SJ (Ed.). Current Directions in Radiopharmaceutical Research and Development. Kluwer Academic Publisher, 1996: 219–232.

[109] Lapchak PA, Araujo DM, Hefti F. Effects of chronic nerve growth factor treatment on hippocampal [^{3}H]cytisine/nicotinic binding sites and presynaptic nicotinic receptor function following fimbrial transections. Neuroscience 1994, 60: 293–298.

[110] Rubboli F, Court JA, Sala C, Morris C, Perry E, Clementi F. Distribution of neuronal nicotinic receptor subunits in human brain. Neurochem Int 1994, 25: 69–71.

[111] Baddick CG, Marks MJ. An autoradiographic survey of mouse brain nicotinic acetylcholine receptors defined by null mutants. Biochem Pharmacol 2011, 82: 828–841.

[112] Morley BJ, Kemp GE, Salvaterra P. α-Bungarotoxin binding sites in the CNS. Life Sci 1979, 24: 859–872.

[113] Whiteaker P, Davies AR, Marks MJ, Blagbrough IS, Potter BV, Wolstenholme AJ*, et al*. An autoradiographic study of the distribution of binding sites for the novel α7-selective nicotinic radioligand [^{3}H]-methyllycaconitine in the mouse brain. Eur J Neurosci 1999, 11: 2689–2696.

[114] Deuther-Conrad W, Fischer S, Hiller A, Nielsen EO, Timmermann DB, Steinbach J*, et al.* Molecular imaging of α7 nicotinic acetylcholine receptors: design and evaluation of the potent radioligand [^{18}F]NS10743. Eur J Nucl Med Mol Imaging 2009, 36: 791–800.

[115] Daly JW. Thirty years of discovering arthropod alkaloids in amphibian skin. J Nat Prod 1998, 61: 162–172.

[116] Avalos M, Parker MJ, Maddox FN, Carroll FI, Luetje CW. Effects of pyridine ring substitutions on affinity, efficacy, and subtype selectivity of neuronal nicotinic receptor agonist epibatidine. J Pharmacol Exp Ther 2002, 302: 1246–1252.

[117] Deuther-Conrad W, Patt JT, Feuerbach D, Wegner F, Brust P, Steinbach J. Norchloro-fluoro-homoepibatidine: specificity to neuronal nicotinic acetylcholine receptor subtypes *in vitro*. Farmaco 2004, 59: 785–792.

[118] Deuther-Conrad W, Patt JT, Lockman PR, Allen DD, Patt M, Schildan A*, et al.* Norchloro-fluoro-homoepibatidine (NCFHEB) - A promising radioligand for neuroimaging nicotinic acetylcholine receptors with PET. Eur Neuropsychopharmacol 2008, 18: 222–229.

[119] Smits R, Fischer S, Hiller A, Deuther-Conrad W, Wenzel B, Patt M*, et al.* Synthesis and biological evaluation of both enantiomers of [^{18}F]flubatine, promising radiotracers with fast kinetics for the imaging of $\alpha_4\beta_2$-nicotinic acetylcholine receptors. Bioorg Med Chem 2014, 22: 804–812.

[120] Patt JT, Spang JE, Westera G, Buck A, Schubiger PA. Synthesis and *in Vivo* studies of [C-11]N-methylepibatidine: comparison of the stereoisomers. Nucl Med Biol 1999, 26: 165–173.

[121] Molina PE, Ding YS, Carroll FI, Liang F, Volkow ND, Pappas N*, et al.* Fluoro-norchloroepibatidine: preclinical assessment of acute toxicity. Nucl Med Biol 1997, 24: 743–747.

[122] Gandiha A, Marshall IG. The effects of 2-(4-phenylpiperidino)-cyclohexanol (AH5183) on the acetylcholine content of, and output from, the chick biventer cervicis muscle preparation. Int J Neurosci 1973, 5: 191–196.

[123] Prior C, Marshall IG, Parsons SM. The pharmacology of vesamicol: an inhibitor of the vesicular acetylcholine transporter. Gen Pharmacol 1992, 23: 1017–1022.

[124] Hicks BW, Rogers GA, Parsons SM. Purification and characterization of a nonvesicular vesamicol-binding protein from electric organ and demonstration of a related protein in mammalian brain. J Neurochem 1991, 57: 509–519.

[125] Kovac M, Mavel S, Deuther-Conrad W, Meheux N, Glockner J, Wenzel B*, et al.* 3D QSAR study, synthesis, and *in vitro* evaluation of (+)-5-FBVM as potential PET radioligand for the vesicular acetylcholine transporter (VAChT). Bioorg Med Chem 2010, 18: 7659–7667.

[126] Mulholland GK, Jung YW, Wieland DM, Kilbourn MR, Kuhl DE. Synthesis of [^{18}F] fluoroethoxy-benzovesamicol, a radiotracer for cholinergic neurons. J Labelled Comp Radiopharm 1993, 33: 583–591.

[127] Petrou M, Frey KA, Kilbourn MR, Scott PJ, Raffel DM, Bohnen NI*, et al*. *In vivo* imaging of human cholinergic nerve terminals with (-)-5-^{18}F-fluoroethoxybenzovesamicol: biodistribution, dosimetry, and tracer kinetic analyses. J Nucl Med 2014. doi:10.2967/jnumed.113.124792.

[128] Parent MJ, Bedard MA, Aliaga A, Minuzzi L, Mechawar N, Soucy JP*, et al.* Cholinergic depletion in Alzheimer's disease shown by [^{18}F]FEOBV autoradiography. Int J Mol Imaging 2013, 2013: 205045.

[129] Szymoszek A, Wenzel B, Scheunemann M, Steinbach J, Schüürmann G. First CoMFA characterization of vesamicol analogs as ligands for the vesicular acetylcholine transporter. J Med Chem 2008, 51: 2128–2136.

[130] Maier CA, Wünsch B. Novel spiropiperidines as highly potent and subtype selective σ-receptor ligands. Part 1. J Med Chem 2002, 45: 438–448.

[131] Maier CA, Wünsch B. Novel s receptor ligands. Part 2. SAR of spiro[[2]benzopyran-1,4'-piperidines] and spiro[[2] benzofuran-1,4'-piperidines] with carbon substituents in position 3. J Med Chem 2002, 45: 4923–4930.

[132] Maier CA, Wünsch B. Novel s receptor ligands, Part 3: Synthesis and SAR studies of 3-substituted 1 '-benzylspiro[[2] benzoxepine-1,4 '-piperidines]. Eur J Org Chem 2003: 714–720.

[133] Große Maestrup E, Fischer S, Wiese C, Schepmann D, Hiller A, Deuther-Conrad W*, et al.* Evaluation of spirocyclic 3-(3-fluoropropyl)-2-benzofurans as σ_1 receptor ligands for neuroimaging with positron emission tomography. J Med Chem 2009, 52: 6062–6072.

[134] Große Maestrup E, Wiese C, Schepmann D, Brust P, Wünsch B. Synthesis, pharmacological activity and structure affinity relationships of spirocyclic σ_1 receptor ligands with a (2-fluoroethyl) residue in 3-position. Bioorg Med Chem 2011, 19: 393–405.

[135] Große Maestrup E, Wiese C, Schepmann D, Hiller A, Fischer S, Scheunemann M*, et al.* Synthesis of spirocyclic sigma(1) receptor ligands as potential PET radiotracers, structure-affinity relationships and *in vitro* metabolic stability. Bioorg Med Chem 2009, 17: 3630–3641.

[136] Holl K, Falck E, Köhler J, Schepmann D, Humpf HU, Brust P*, et al.* Synthesis, characterization, and metabolism studies of fluspidine enantiomers. Chem Med Chem 2013, 8: 2047–2056.

[137] Maisonial A, Grosse Maestrup E, Fischer S, Hiller A, Scheunemann M, Wiese C*, et al.* A ^{18}F-labeled fluorobutyl-substituted spirocyclic piperidine derivative as a selective radioligand for PET Imaging of σ_1 receptors. Chem Med Chem 2011, 6: 1401–1410.

[138] Maisonial A, Grosse Maestrup E, Wiese C, Hiller A, Schepmann D, Fischer S*, et al.* Synthesis, radiofluorination and pharmacological evaluation of a fluoromethyl spirocyclic PET tracer for central σ_1 receptors and comparison with fluoroalkyl homologs. Bioorg Med Chem 2012, 20: 257–269.

[139] Fischer S, Wiese C, Grosse Maestrup E, Hiller A, Deuther-Conrad W, Scheunemann M*, et al.* Molecular imaging of sigma receptors: synthesis and evaluation of the potent σ_1 selective radioligand [^{18}F]fluspidine. Eur J Nucl Med Mol Imaging 2011, 38: 540–551.

[140] Bickel U. How to measure drug transport across the blood-brain barrier. NeuroRx 2005, 2: 15–26.

[141] Pardridge WM. Drug transport across the blood-brain barrier. J Cereb Blood Flow Metab 2012, 32: 1959–1972.

[142] Kessler RM, Ansari MS, de Paulis T, Schmidt DE, Clanton JA, Smith HE*, et al.* High affinity dopamine D_2 receptor radioligands. 1. Regional rat brain distribution of iodinated benzamides. J Nucl Med 1991, 32: 1593–1600.

[143] Tsuji A. Small molecular drug transfer across the blood-brain barrier via carrier-mediated transport systems. NeuroRx 2005, 2: 54–62.

[144] Ecker GF, Noe CR. In silico prediction models for blood-brain barrier permeation. Curr Med Chem 2004, 11: 1617–1628.

[145] Gouverneur V, Müller K. Fluorine in Pharmaceutical and Medicinal Chemistry: From Biophysical Aspects to Clinical Applications. Singapore: World Scientific Publishing 2012.

[146] Tressaud A, Haufe G (Eds.). Fluorine and Health, Molecular Imaging, Biomedical Materials and Pharmaceuticals. Elsevier Science, 2008.

[147] Alauddin MM. Positron emission tomography (PET) imaging with ^{18}F-based radiotracers. Am J Nucl Med Mol Imaging 2012, 2: 55–76.

[148] Ross TL, Wester HJ. ^{18}F: Labeling chemistry and labeled compounds. In: Vértes A, Nagy S, Klencsár Z, Lovas R, Rösch F (Eds.). Handbook of Nuclear Chemistry: Radiochemistry and Radiopharmaceutical Chemistry in Life Sciences, 2nd Ed. Springer, 2011, 4: 2021–2071.

[149] Schubiger PA, Lehmann L, Friebe M. PET Chemistry: The Driving Force in Molecular Imaging. Springer, 2007.

[150] Bergman J, Solin O. Fluorine-18-labeled fluorine gas for synthesis of tracer molecules. Nucl Med Biol 1997, 24: 677–683.

[151] Forsback S, Marjamäki P, Eskola O, Bergman J, Rokka J, Grönroos T*, et al.* [^{18}F]CFT synthesis and binding to monoamine transporters in rats. EJNMMI Res 2012, 2: 3.

[152] Ermisch A, Brust P, Kretzschmar R, Rühle HJ. Peptides and Blood-Brain Barrier Transport. Physiol Rev 1993, 73: 489–527.

[153] Coenen HH, Hamacher K, Schüller M, Stöcklin G, Klatte B, Knöchel A. Process for the preparation of fluorine-18 labelled compounds by nucleophilic exchange. EP0167103 A2, 1985.

[154] Coenen HH, Colosimo M, Schüller M, Stöcklin G. Preparation of n.c.a. [^{18}F]CH_2BrF via aminopolyether supported nucleophilic substitution. J Labelled Compd Radiopharm 1986, 23: 587–595.

[155] Roeda D, Dolle F. Aliphatic nucleophilic radiofluorination. Curr Radiopharm 2010, 3: 81–108

[156] Cai LS, Lu SY, Pike VW. Chemistry with [^{18}F]fluoride ion. European J Org Chem 2008: 2853–2873.

[157] Hoepping A, Scheunemann M, Fischer S, Deuther-Conrad W, Hiller A, Wegner F*, et al.* Radiosynthesis and biological evaluation of an ^{18}F-labeled derivative of the novel pyrazolopyrimidine sedative-hypnotic agent indiplon. Nucl Med Biol 2007, 34: 559–570.

[158] Deuther-Conrad W, Fischer S, Scheunemann M, Hiller A, Diekers M, Friemel A*, et al.* $GABA_A$ receptor specific pyrazolopyrimidines as potential imaging agents: *In vivo* characteristics of a new ^{18}F-labelled Indiplon derivative. Curr Radiopharm 2009, 2: 24–31.

[159] Fischer S, Hiller A, Scheunemann M, Deuther-Conrad W, Hoepping A, Diekers M*, et al.* Radiosynthesis of novel ^{18}F-labelled derivatives of indiplon as potential $GABA_A$ receptor imaging tracers for PET. J Labelled Comp Radiopharm 2008, 51: 123–131.

[160] Schirrmacher R, Bradtmöller G, Schirrmacher E, Thews O, Tillmanns J, Siessmeier T*, et al.* ^{18}F-labeling of peptides by means of an organosilicon-based fluoride acceptor. Angew Chem Int Ed Engl 2006, 45: 6047–6050.

[161] Römer J, Füchtner F, Steinbach J, Kasch H. Automated synthesis of 16α-[^{18}F]fluoroestradiol-3,17β-disulphamate. Appl Radiat Isot 2001, 55: 631–639.

[162] Ermert J, Coenen HH. Nucleophilic ^{18}F-fluorination of complex molecules in activated carbocyclic aromatic position. Curr Radiopharm 2010, 3: 109–126

[163] Fischer S, Hiller A, Smits R, Hoepping A, Funke U, Wenzel B*, et al.* Radiosynthesis of racemic and enantiomerically pure (-)-[^{18}F]flubatine-A promising PET radiotracer for neuroimaging of $\alpha_4\beta_2$ nicotinic acetylcholine receptors. Appl Radiat Isot 2013, 74C: 128–136.

[164] Patt JT, Deuther-Conrad W, Wohlfarth K, Feuerbach D, Brust P, Steinbach J. Norchloro-fluoro-homoepibatidine: ^{18}F-labelling and evaluation of affinity and selectivity at neuronal nicotinic acetylcholine receptors. J Labelled Compd Radiopharm 2003, 46 (S1): S 168.

[165] Patt M, Schildan A, Habermann B, Fischer S, Hiller A, Deuther-Conrad W*, et al.* Fully automated radiosynthesis of both enantiomers of [^{18}F]Flubatine under GMP conditions for human application. Appl Radiat Isot 2013, 80: 7–11.

[166] Hockley BG, Stewart MN, Sherman P, Quesada C, Kilbourn MR, Albin RL*, et al.* (-)-[^{18}F]Flubatine: evaluation

in rhesus monkeys and a report of the first fully automated radiosynthesis validated for clinical use. J Labelled Comp Radiopharm 2013, 56: 595–599.

[167] Rühl T, Deuther-Conrad W, Fischer S, Günther R, Hennig L, Krautscheid H*, et al.* Cannabinoid receptor type 2 (CB_2)-selective N-aryl-oxadiazolyl-propionamides: synthesis, radiolabelling, molecular modelling and biological evaluation. Org Med Chem Lett 2012, 2: 32.

[168] Teodoro R, Moldovan RP, Lueg C, Günther R, Donat CK, Ludwig FA*, et al.* Radiofluorination and biological evaluation of *N*-aryl-oxadiazolyl-propionamides as potential radioligands for PET imaging of cannabinoid CB_2 receptors. Org Med Chem Lett 2013, 3: 11.

[169] Löser R, Fischer S, Hiller A, Köckerling M, Funke U, Maisonial A*, et al.* Use of 3-[^{18}F]fluoropropanesulfonyl chloride as a prosthetic agent for the radiolabelling of amines: Investigation of precursor molecules, labelling conditions and enzymatic stability of the corresponding sulfonamides. Beilstein J Org Chem 2013, 9: 1002–1011.

[170] Wüst F, Köhler L, Berndt M, Pietzsch J. Systematic comparison of two novel, thiol-reactive prosthetic groups for ^{18}F labeling of peptides and proteins with the acylation agent succinimidyl-4-[^{18}F]fluorobenzoate ([^{18}F]SFB). Amino Acids 2009, 36: 283–295.

[171] Serdons K, Verbruggen A, Bormans GM. Developing new molecular imaging probes for PET. Methods 2009, 48: 104–111.

[172] Pretze M, Kuchar M, Bergmann R, Steinbach J, Pietzsch J, Mamat C. An efficient bioorthogonal strategy using CuAAC click chemistry for radiofluorinations of SNEW peptides and the role of copper depletion. Chem Med Chem 2013, 8: 935–945.

[173] Pretze M, Pietzsch D, Mamat C. Recent trends in bioorthogonal click-radiolabeling reactions using fluorine-18. Molecules 2013, 18: 8618–8665.

[174] Ramenda T, Kniess T, Bergmann R, Steinbach J, Wüst F. Radiolabelling of proteins with fluorine-18 via click chemistry. Chem Commun (Camb) 2009: 7521–7523.

[175] Ramenda T, Steinbach J, Wüst F. 4-[^{18}F]Fluoro-N-methyl-N-(propyl-2-yn-1-yl)benzenesulfonamide ([^{18}F]F-SA): a versatile building block for labeling of peptides, proteins and oligonucleotides with fluorine-18 via Cu(I)-mediated click chemistry. Amino Acids 2013, 44: 1167–1180.

[176] Kniess T, Laube M, Bergmann R, Sehn F, Graf F, Steinbach J*, et al.* Radiosynthesis of a ^{18}F-labeled 2,3-diarylsubstituted indole via McMurry coupling for functional characterization of cyclooxygenase-2 (COX-2) *in vitro* and *in vivo*. Bioorg Med Chem 2012, 20: 3410–3421.

[177] Funke U, Fischer S, Hiller A, Scheunemann M, Deuther-Conrad W, Brust P*, et al.* 3-(4-(6-Fluoroalkoxy-3,4-dihydroisoquinoline-2(1H)-yl)cyclohexyl)-1H-indol e-5-carbonitriles for SERT imaging: chemical synthesis, evaluation *in vitro* and radiofluorination. Bioorg Med Chem Lett 2008, 18: 4727–4730.

[178] Funke U, Schwan G, Maisonial A, Scheunemann M, Deuther-Conrad W, Fischer S*, et al.* Radiosynthesis and radiotracer properties of a 7-(2-[^{18}F]fluoroethoxy)-6-methoxy-pyrrolidinylquinazoline for imaging of phosphodiesterase 10A with PET. Pharmaceuticals (Basel) 2012, 5: 169–188.

[179] Sorger D, Scheunemann M, Grossmann U, Fischer S, Vercouille J, Hiller A*, et al.* A new ^{18}F-labeled fluoroacetylmorpholino derivative of vesamicol for neuroimaging of the vesicular acetylcholine transporter. Nucl Med Biol 2008, 35: 185–195.

[180] Hoepping A, Scheunemann M, Fischer S, Deuther-Conrad W, Hiller A, Wegner F*, et al.* Radiosynthesis and biological evaluation of an ^{18}F-labeled derivative of the novel pyrazolopyrimidine sedative-hypnotic agent indiplon. Nucl Med Biol 2007, 34: 559–570.

[181] Donat CK, Schuhmann MU, Voigt C, Nieber K, Deuther-Conrad W, Brust P. Time-dependent alterations of cholinergic markers after experimental traumatic brain injury. Brain Res 2008, 1246: 167–177.

[182] Perry DC, Kellar KJ. [^{3}H]epibatidine labels nicotinic receptors in rat brain: an autoradiographic study. J Pharmacol Exp Ther 1995, 275: 1030–1034.

[183] Vaupel DB, Mukhin AG, Kimes AS, Horti AG, Koren AO, London ED. *In vivo* studies with [125I]5-I-A-85380, a nicotinic acetylcholine receptor radioligand. Neuroreport 1998, 9: 2311–2317.

[184] Davies AR, Hardick DJ, Blagbrough IS, Potter BV, Wolstenholme AJ, Wonnacott S. Characterisation of the binding of [^{3}H]methyllycaconitine: a new radioligand for labelling α7-type neuronal nicotinic acetylcholine receptors. Neuropharmacology 1999, 38: 679–690.

[185] No-authors-listed. Indiplon. Indiplon modified-release, indiplon MR, NBI 34060, NBI 34060 modified-release, NBI 34060 MR. Drugs R D 2002, 3: 197–199.

[186] Hoepping A, Diekers M, Deuther-Conrad W, Scheunemann M, Fischer S, Hiller A*, et al.* Synthesis of fluorine substituted pyrazolopyrimidines as potential leads for the development of PET-imaging agents for the GABAA receptors. Bioorg Med Chem 2008, 16: 1184–1194.

[187] Brust P, Scheffel U, Szabo Z. Radioligands for the study of the 5-HT transporter *in vivo*. IDrugs 1999, 2: 129–145.

[188] Kretzschmar M, Brust P, Zessin J, Cumming P, Bergmann R, Johannsen B. Autoradiographic imaging of the serotonin transporter in the brain of rats and pigs using S-([^{18}F] Fluoromethyl)-(+)-McN5652. Eur Neuropsychopharmacol 2003, 13: 387–397.

[189] Kung MP, Stevenson DA, Plössl K, Meegalla SK, Beckwith A, Essman WD, *et al.* [^{99m}Tc]TRODAT-1: a novel technetium-99m complex as a dopamine transporter imaging agent. European J Nucl Med 1997, 24: 372–380.

[190] Kung HF, Kung MP, Wey SP, Lin KJ, Yen TC. Clinical acceptance of a molecular imaging agent: a long march with [Tc-99m]TRODAT. Nucl Med Biol 2007, 34: 787–789.

[191] Tan PZ, Baldwin RM, Van Dyck CH, Al-Tikriti M, Roth B, Khan N, *et al.* Characterization of radioactive metabolites of 5-HT_{2A} receptor PET ligand [^{18}F]altanserin in human and rodent. Nucl Med Biol 1999, 26: 601–608.

[192] van Dyck CH, Tan PZ, Baldwin RM, Amici LA, Garg PK, Ng CK, *et al.* PET quantification of 5-HT2A receptors in the human brain: a constant infusion paradigm with [^{18}F] altanserin. J Nucl Med 2000, 41: 234–241.

[193] Liptrot M, Adams KH, Martiny L, Pinborg LH, Lonsdale MN, Olsen NV, *et al.* Cluster analysis in kinetic modelling of the brain: a noninvasive alternative to arterial sampling. Neuroimage 2004, 21: 483–493.

[194] Bergström KA, Halldin C, Kuikka JT, Swahn CG, Tiihonen J, Hiltunen J, *et al.* Lipophilic metabolite of [^{123}I]β-CIT in human plasma may obstruct quantitation of the dopamine transporter. Synapse 1995, 19: 297–300.

[195] Lundkvist C, Halldin C, Swahn CG, Ginovart N, Farde L. Different brain radioactivity curves in a PET study with [^{11}C] β-CIT labelled in two different positions. Nucl Med Biol 1999, 26: 343–350.

[196] Zoghbi SS, Shetty HU, Ichise M, Fujita M, Imaizumi M, Liow JS, *et al.* PET imaging of the dopamine transporter with ^{18}F-FECNT: a polar radiometabolite confounds brain radioligand measurements. J Nucl Med 2006, 47: 520–527.

[197] Shetty HU, Zoghbi SS, Liow JS, Ichise M, Hong J, Musachio JL, *et al.* Identification and regional distribution in rat brain of radiometabolites of the dopamine transporter PET radioligand [^{11}C]PE2I. Eur J Nucl Med Mol Imaging 2007, 34: 667–678.

[198] Peyronneau MA, Saba W, Dolle F, Goutal S, Coulon C, Bottlaender M, *et al.* Difficulties in dopamine transporter radioligand PET analysis: the example of LBT-999 using [^{18}F] and [^{11}C] labelling: part II: Metabolism studies. Nucl Med Biol 2012, 39: 347–359.

[199] Bergström KA, Halldin C, Hall H, Lundkvist C, Ginovart N, Swahn CG, *et al. In vitro* and *in vivo* characterisation of nor-β-CIT: a potential radioligand for visualisation of the serotonin transporter in the brain. European J Nucl Med 1997, 24: 596–601.

[200] Guengerich FP. Common and uncommon cytochrome P450 reactions related to metabolism and chemical toxicity. Chem Res Toxicol 2001, 14: 611–650.

[201] Carroll FI, Blough BE, Nie Z, Kuhar MJ, Howell LL, Navarro HA. Synthesis and monoamine transporter binding properties of 3beta-(3',4'-disubstituted phenyl)tropane-2beta-carboxylic acid methyl esters. J Med Chem 2005, 48: 2767–2771.

[202] Mori T, Sun LQ, Kobayashi M, Kiyono Y, Okazawa H, Furukawa T, *et al.* Preparation and evaluation of ethyl [^{18}F] fluoroacetate as a proradiotracer of [^{18}F]fluoroacetate for the measurement of glial metabolism by PET. Nucl Med Biol 2009, 36: 155–162.

[203] Dienel GA, Popp D, Drew PD, Ball K, Krisht A, Cruz NF. Preferential labeling of glial and meningial brain tumors with [2-^{14}C]acetate. J Nucl Med 2001, 42: 1243–1250.

[204] Lear JL, Ackermann RF. Evaluation of radiolabeled acetate and fluoroacetate as potential tracers of cerebral oxidative metabolism. Metab Brain Dis 1990, 5: 45–56.

[205] Davson H, Segal MB. Physiology of the CSF and Blood-Brain Barriers. Boca Raton, USA: CRC Press, 1996.

[206] Rogers GA, Stone-Elander S, Ingvar M, Eriksson L, Parsons SM, Widen L. ^{18}F-labelled vesamicol derivatives: syntheses and preliminary *in vivo* small animal positron emission tomography evaluation. Nucl Med Biol 1994, 21: 219–230.

[207] Tu LQ, Wright PF, Rix CJ, Ahokas JT. Is fluoroacetate-specific defluorinase a glutathione S-transferase? Comp Biochem Physiol C Toxicol Pharmacol 2006, 143: 59–66.

[208] Johnson JA, el Barbary A, Kornguth SE, Brugge JF, Siegel FL. Glutathione S-transferase isoenzymes in rat brain neurons and glia. J Neurosci 1993, 13: 2013–2023.

[209] Brust P, Hinz R, Kuwabara H, Hesse S, Zessin J, Pawelke B, *et al. In vivo* measurement of the serotonin transporter with (S)-([^{18}F]fluoromethyl)-(+)-McN5652. Neuropsychopharmacology 2003, 28: 2010–2019.

[210] Hesse S, Brust P, Mäding P, Becker GA, Patt M, Seese A, *et al.* Imaging of the brain serotonin transporters (SERT) with ^{18}F-labelled fluoromethyl-McN5652 and PET in humans. Eur J Nucl Med Mol Imaging 2012, 39: 1001–1011.

[211] Szabo Z, Scheffel U, Mathews WB, Ravert HT, Szabo K, Kraut M, *et al.* Kinetic analysis of [^{11}C]McN5652: a serotonin transporter radioligand. J Cereb Blood Flow Metab 1999, 19: 967–981.

[212] Brust P, Patt JT, Deuther–Conrad W, Becker G, Patt M, Schildan A, *et al. In vivo* measurement of nicotinic acetylcholine receptors with [^{18}F]norchloro-fluoro-homoepibatidine. Synapse 2008, 62: 205–218.

[213] Patt M, Becker GA, Grossmann U, Habermann B, Schildan A, Wilke S, *et al.* Evaluation of metabolism, plasma protein binding and other biological parameters after administration of (-)-[^{18}F]flubatine in humans. Nucl Med Biol 2014. doi. org/10.1016/j.nucmedbio.2014.1003.1018.

[214] Becker GA, Wilke S, Schönknecht P, Patt M, Luthardt J, Hesse S, *et al.* Comparison of (-)-[^{18}F]-flubatine and 2-[^{18}F] FA-85380 binding to nicotinic alpha4beta2 acetylcholine receptors in human brains. Eur J Nucl Med Mol Imaging

2013, 40 (Suppl. 2): S271.

[215] Fasinu P, Bouic PJ, Rosenkranz B. Liver-based *in vitro* technologies for drug biotransformation studies - a review. Curr Drug Metab 2012, 13: 215–224.

[216] Davydov DR. Microsomal monooxygenase as a multienzyme system: the role of P450-P450 interactions. Expert Opin Drug Metab Toxicol 2011, 7: 543–558.

[217] Stabin MG. Fundamentals of Nuclear Medicine Dosimetry. Springer, 2008.

[218] van de Waterbeemd H, Camenisch G, Folkers G, Chretien JR, Raevsky OA. Estimation of blood-brain barrier crossing of drugs using molecular size and shape, and H-bonding descriptors. J Drug Target 1998, 6: 151–165.

[219] Ball K, Bouzom F, Scherrmann JM, Walther B, Decleves X. Physiologically based pharmacokinetic modelling of drug penetration across the blood-brain barrier-towards a mechanistic IVIVE-based approach. AAPS J 2013, 15: 913–932.

[220] Shawahna R, Decleves X, Scherrmann JM. Hurdles with using *in vitro* models to predict human blood-brain barrier drug permeability: a special focus on transporters and metabolizing enzymes. Curr Drug Metab 2013, 14: 120–136.

[221] Uchida Y, Ohtsuki S, Katsukura Y, Ikeda C, Suzuki T, Kamiie J*, et al.* Quantitative targeted absolute proteomics of human blood-brain barrier transporters and receptors. J Neurochem 2011, 117: 333–345.

[222] Rötering S, Scheunemann M, Fischer S, Hiller A, Peters D, Deuther-Conrad W*, et al.* Radiosynthesis and first evaluation in mice of [^{18}F]NS14490 for molecular imaging of α7 nicotinic acetylcholine receptors. Bioorg Med Chem 2013, 21: 2635–2642.

[223] Syvänen S, Lindhe O, Palner M, Kornum BR, Rahman O, Langström B*, et al.* Species differences in blood-brain barrier transport of three positron emission tomography radioligands with emphasis on P-glycoprotein transport. Drug Metab Dispos 2009, 37: 635–643.

[224] Wagner HN, Jr., Burns HD, Dannals RF, Wong DF, Langström B, Duelfer T*, et al.* Imaging dopamine receptors in the human brain by positron tomography. Science 1983, 221: 1264–1266.

[225] Ehrin E, Farde L, de Paulis T, Eriksson L, Greitz T, Johnström P*, et al.* Preparation of ^{11}C-labelled Raclopride, a new potent dopamine receptor antagonist: preliminary PET studies of cerebral dopamine receptors in the monkey. Int J Appl Radiat Isot 1985, 36: 269–273.

[226] Chan GL, Holden JE, Stoessl AJ, Doudet DJ, Wang Y, Dobko T*, et al.* Reproducibility of the distribution of carbon-11-SCH 23390, a dopamine D_1 receptor tracer, in normal subjects. J Nucl Med 1998, 39: 792–797.

[227] Parsey RV, Arango V, Olvet DM, Oquendo MA, Van Heertum RL, John Mann J. Regional heterogeneity of 5-HT_{1A} receptors in human cerebellum as assessed by positron emission tomography. J Cereb Blood Flow Metab 2005, 25: 785–793.

[228] Biver F, Goldman S, Luxen A, Monclus M, Forestini M, Mendlewicz J*, et al.* Multicompartmental study of F-18 altanserin binding to brain $5HT_2$ receptors in humans using positron emission tomography. Eur J Nucl Med 1994, 21: 937–946.

[229] Itoh T, Tanaka M, Kobayashi K, Suzuki K, Inoue O. Binding kinetics of ^{11}C-N-methyl piperidyl benzilate (^{11}C-NMPB) in a rhesus monkey brain using the cerebellum as a reference region. Ann Nucl Med 2005, 19: 499–505.

[230] Deuther-Conrad W, Fischer S, Hiller A, Becker G, Cumming P, Xiong G*, et al.* Assessment of α7 nicotinic acetylcholine receptor availability in porcine brain with [^{18}F]NS10743. Eur J Nucl Med Mol Imaging 2011, 38: 1541–1549.

[231] Flesher JE, Scheffel U, London ED, Frost JJ. *In vivo* labeling of nicotinic cholinergic receptors in brain with [^{3}H]cytisine. Life Sci 1994, 54: 1883–1890.

[232] Ishiwata K, Kawamura K, Wang WF, Tsukada H, Harada N, Mochizuki H*, et al.* Evaluation of *in vivo* selective binding of [^{11}C]doxepin to histamine H_1 receptors in five animal species. Nucl Med Biol 2004, 31: 493–502.

[233] Kish SJ, Furukawa Y, Chang LJ, Tong J, Ginovart N, Wilson A*, et al.* Regional distribution of serotonin transporter protein in postmortem human brain: Is the cerebellum a SERT-free brain region? Nucl Med Biol 2005, 32: 123–128.

[234] Brust P, Hesse S, Müller U, Szabo Z. Neuroimaging of the serotonin transporter - possibilities and pitfalls. Curr Psychiat Rev 2006, 2: 111–149.

[235] Marjamäki P, Zessin J, Eskola O, Grönroos T, Haaparanta M, Bergman J*, et al.* S-[^{18}F]fluoromethyl-(+)-McN5652, a PET tracer for the serotonin transporter: Evaluation in rats. Synapse 2003, 47: 45–53.

[236] Deuther-Conrad W, Maisonial A, Patt M, Stittsworth S, Becker G, Habermann B*, et al.* Discovery of enantioselective suitability of (R)-(+)- and (S)-(-)-[^{18}F]fluspidine for σ_1 receptor imaging. J Label Comp Radiopharm 2013, 56: S55.

[237] Brust P, Deuther-Conrad W, Becker G, Patt M, Donat CK, Stittsworth S*, et al.* Distinctive *in vivo* kinetics of the new sigma1 receptor ligands (R)-(+)- and (S)-(-)-^{18}F-fluspidine in porcine brain. J Nucl Med 2014, pii: jnumed.114.137562.

[238] Leenders KL, Gibbs JM, Frackowiak RS, Lammertsma AA, Jones T. Positron emission tomography of the brain: new possibilities for the investigation of human cerebral pathophysiology. Prog Neurobiol 1984, 23: 1–38.

[239] Mintun MA, Raichle ME, Kilbourn MR, Wooten GF, Welch MJ. A quantitative model for the *in vivo* assessment of drug binding sites with positron emission tomography. Ann Neurol 1984, 15: 217–227.

[240] Miyoshi S, Mitsuoka K, Nishimura S, Veltkamp SA. Radioisotopes in Drug Research and Development: Focus on Positron Emission Tomography. In: Singh N (Ed). Radioisotopes - Applications in Bio-Medical Science. InTech, 2011: 93–113.

[241] Yanai K, Ido T, Ishiwata K, Hatazawa J, Watanuki S, Takahashi T, *et al.* Characteristics of specific *in vivo* labeling of neuroleptic binding sites with 3-N-[^{11}C]methylspiperone. European J Nucl Med 1986, 11: 438–443.

[242] Brust P, Shaya EK, Jeffries KJ, Dannals RF, Ravert HT, Wilson AA*, et al.* Effects of vasopressin on blood-brain transfer of methionine in dogs. J Neurochem 1992, 59: 1421–1429.

[243] Kong FL, Ford RJ, Yang DJ. Managing lymphoma with non-FDG radiotracers: current clinical and preclinical applications. Biomed Res Int 2013, 2013: 626910.

[244] Prenen GH, Go KG, Paans AM, Zuiderveen F, Vaalburg W, Kamman RL*, et al.* Positron emission tomographical studies of 1-^{11}C-acetoacetate, 2-^{18}F-fluoro-deoxy-D-glucose, and L-1-^{11}C-tyrosine uptake by cat brain with an experimental lesion. Acta Neurochirurgica 1989, 99: 166–172.

[245] Ginovart N, Wilson AA, Meyer JH, Hussey D, Houle S. [^{11}C]-DASB, a tool for *in vivo* measurement of SSRI-induced occupancy of the serotonin transporter: PET characterization and evaluation in cats. Synapse 2003, 47: 123–133.

[246] Bauer R, Bergmann R, Beyer GJ, Manfrass P, Steinbach J, Kretzschmar M*, et al.* Investigations of cerebral glucose utilization into the newborn brain: a [^{18}F]-FDG positron emission tomography study using a high resolution multiwire proportional chamber detector device. Exp Pathol 1991, 42: 229–233.

[247] Sauleau P, Lapouble E, Val-Laillet D, Malbert CH. The pig model in brain imaging and neurosurgery. Animal 2009, 3: 1138–1151.

[248] Alstrup AKO, Smith DF. PET neuroimaging in pigs. Scand J Lab Anim Sci 2012, 39: 25–45.

[249] Herzog H. PET/MRI: challenges, solutions and perspectives. Z Med Phys 2012, 22: 281–298.

[250] Herzog H, van den Hoff J. Combined PET/MR systems: an overview and comparison of currently available options. Q J Nucl Med Mol Imaging 2012, 56: 247–267.

[251] Xi W, Tian M, Zhang H. Molecular imaging in neuroscience research with small-animal PET in rodents. Neurosci Res 2011, doi:10.1016/j.neures.2010.12.017.

[252] Lancelot S, Zimmer L. Small-animal positron emission tomography as a tool for neuropharmacology. Trends Pharmacol Sci 2010, 31: 411–417.

[253] Syvänen S, Labots M, Tagawa Y, Eriksson J, Windhorst AD, Lammertsma AA*, et al.* Altered $GABA_A$ receptor density and unaltered blood-brain barrier transport in a kainate model of epilepsy: an *in vivo* study using ^{11}C-flumazenil and PET. J Nucl Med 2012, 53: 1974–1983.

[254] Gunn RN, Gunn SR, Turkheimer FE, Aston JA, Cunningham VJ. Positron emission tomography compartmental models: a basis pursuit strategy for kinetic modeling. J Cereb Blood Flow Metab 2002, 22: 1425–1439.

[255] Schmidt KC, Turkheimer FE. Kinetic modeling in positron emission tomography. Quarterly J Nucl Med 2002, 46: 70–85.

[256] Laruelle M, Slifstein M, Huang Y. Positron emission tomography: imaging and quantification of neurotransporter availability. Methods 2002, 27: 287–299.

[257] Watabe H, Ikoma Y, Kimura Y, Naganawa M, Shidahara M. PET kinetic analysis--compartmental model. Ann Nucl Med 2006, 20: 583–588.

[258] van den Hoff J. Principles of quantitative positron emission tomography. Amino Acids 2005, 29: 341–353.

[259] van den Hoff J. Kinetic Modelling. In: Kiessling F, Pichler BJ. Small Animal Imaging: Basics and Practical Guide. Springer, 2010: 387–404.

[260] Brust P, Zessin J, Kuwabara H, Pawelke B, Kretzschmar M, Hinz R*, et al.* Positron emission tomography imaging of the serotonin transporter in the pig brain using [^{11}C](+)-McN5652 and S-([^{18}F]fluoromethyl)-(+)-McN5652. Synapse 2003, 47: 143–151.

[261] Lammertsma AA, Bench CJ, Hume SP, Osman S, Gunn K, Brooks DJ*, et al.* Comparison of methods for analysis of clinical C-11 raclopride studies. J Cereb Blood Flow Metab 1996, 16: 42–52.

[262] Lammertsma AA, Hume SP. Simplified reference tissue model for PET receptor studies. Neuroimage 1996, 4: 153–158.

[263] Wang G, Qi J. Direct estimation of kinetic parametric images for dynamic PET. Theranostics 2013, 3: 802–815.

[264] Patlak CS, Blasberg RG, Fenstermacher JD. Graphical evaluation of blood-to-brain transfer constants from multiple-time uptake data. J Cereb Blood Flow Metab 1983, 3: 1–7.

[265] Patlak CS, Blasberg RG. Graphical evaluation of blood-to-brain transfer constants from multiple-time uptake data. Generalizations. J Cereb Blood Flow Metab 1985, 5: 584–590.

[266] Gjedde A. High-and low-affinity transport of D-glucose from blood to brain. J Neurochem 1981, 36: 1463–1471.

[267] Logan J, Fowler JS, Volkow ND, Wolf AP, Dewey SL, Schlyer DJ*, et al.* Graphical analysis of reversible radioligand binding from time-activity measurements applied to [N-^{11}C-methyl]-(-)-cocaine PET studies in human subjects. J Cereb Blood Flow Metab 1990, 10: 740–747.

[268] Wang JZ, Qiu P, Liu RKJ, Szabo Z. Model-Based receptor quantization analysis for PET parametric imaging. Conf Proc IEEE Eng Med Biol Soc 2005, 6: 5908–5911.

[269] Dennan S, Decristoforo Ce. The Radiopharmacy. A Technologist's Guide. European Association of Nuclear Medicine,

2008.

[270] Elsinga P, Todde S, Penuelas I, Meyer G, Farstad B, Faivre-Chauvet A*, et al.* Guidance on current good radiopharmacy practice (cGRPP) for the small-scale preparation of radiopharmaceuticals. Eur J Nucl Med Mol Imaging 2010, 37: 1049–1062.

[271] Verbruggen A, Coenen HH, Deverre JR, Guilloteau D, Langstrom B, Salvadori PA*, et al.* Guideline to regulations for radiopharmaceuticals in early phase clinical trials in the EU. Eur J Nucl Med Mol Imaging 2008, 35: 2144–2151.

[272] Zessin J, Eskola O, Steinbach J, Bergman J, Marjamäki P, Brust P*, et al.* Synthesis and first biological evaluation of the [^{18}F]fluormethyl-analog of (+)-MCN5652, a tracer for imaging the serotonin transporter. Nuklearmedizin 2000, 39: A36. [Article in German language]

[273] Petrou M, Koeppe R, Scott P, Bohnen N, Kilbourn M, Frey K. PET imaging of the vesicular acetylcholine transporter. J Nucl Med 2012, 53 (Supplement 1): 290.

[274] Farde L, Ehrin E, Eriksson L, Greitz T, Hall H, Hedström CG*, et al.* Substituted benzamides as ligands for visualization of dopamine receptor binding in the human brain by positron emission tomography. Proc Natl Acad Sci U S A 1985, 82: 3863–3867.

[275] Maziere M, Hantraye P, Prenant C, Sastre J, Comar D. Synthesis of ethyl 8-fluoro-5,6-dihydro-5-[^{11}C]methyl-6-oxo-4H-imidazo [1,5-a] [1,4]benzodiazepine-3-carboxylate (RO 15.1788-11C): a specific radioligand for the *in vivo* study of central benzodiazepine receptors by positron emission tomography. Int J Appl Radiat Isot 1984, 35: 973–976.

[276] Rowland DJ, Cherry SR. Small-animal preclinical nuclear medicine instrumentation and methodology. Semin Nucl Med 2008, 38: 209–222.